UPPSALA
UNIVERSITET

UPTEC W 22020
Examensarbete 30 hp
Juni 2022

Improved Understanding of Water Balance in the Malwathu Oya River Basin Using SWAT and Remote Sensing

Alexander Fors

Abstract

Improved Understanding of Water Balance in the Malwathu Oya River Basin Using SWAT and Remote Sensing
Alexander Fors

As the need for climatic data is increasing in times of climate change and water scarcity, remote sensing (RS) and hydrological modelling are ways to battle these problems, especially in data scarce areas. The actual evapotranspiration (ET_a) is one of the key parameters when assessing the water balance and a good estimate of this parameter is thus of great importance. In this study a hydrological model was created with the Soil and Water Assessment Tool (SWAT) over the Malwathu Oya river basin, Sri Lanka, and the SWAT ET_a estimates were compared to RS derived ET_a from FAO's open access database WaPOR. A sensitivity analysis and a calibration with observed streamflow data of the SWAT model was conducted with the SUFI-2 algorithm in SWAT-CUP. The calibration was satisfactory and showed the following values for the performance parameters: R^2 = 0.72, Nash-Sutcliffe Efficiency, NSE = 0.69, and Percent of Bias, PBIAS = -10.4. The most sensitive parameters were CN2 (runoff curve number for moisture condition II), SOL_AWC (soil available water capacity), and ESCO (soil evaporation compensation factor). The water balance partitioning from the calibrated SWAT model showed a ratio of 0.68 between ET_a and precipitation as an annual average between 2012–2020.

In the comparison between SWAT ET_a and WaPOR ET_a the SWAT ET_a showed a clear underestimation, particularly during the drier *Yala* growing season (May – August). However, the SWAT land use classes representing the cultivated rice fields agreed well with WaPOR while the forest and range grasses were underpredicted. To increase the performance of SWAT in estimating ET_a the following was recommended: improvement of the simulation of the shallow aquifers, more accurate forest parameters, deactivation of the default dormancy period in SWAT, calibration with ET_a instead of streamflow, and a higher resolution soil map together with more soil measurements.

Keywords: actual evapotranspiration, Malwathu Oya, remote sensing, Sri Lanka, SWAT modelling, SWAT calibration, WaPOR, water balance

Department for Soil and Environment, Swedish University of Agricultural Sciences (SLU), Lennart Hjelms väg 9, SE 75007, Uppsala, Sweden. ISSN 1401-5765

Referat

Förbättrad förståelse av vattenbalansen i Malwathu Oyas avrinningsområde med hjälp av SWAT och fjärranalys
Alexander Fors

Eftersom behovet av klimatdata ökar i tider av klimatförändringar och vattenbrist är fjärranalys (RS) och hydrologisk modellering exempel på metoder för att lösa dessa problem, särskilt i områden med brist på data. Den faktiska evapotranspirationen (ET_a) är en nyckelparameter vid bedömning av vattenbalansen och en bra uppskattning av denna parameter är därför av stor betydelse. I denna studie skapades en hydrologisk modell med Soil and Water Assessment Tool (SWAT) över avrinningsområdet Malwathu Oya i Sri Lanka, och SWAT ET_a -uppskattningarna jämfördes med RS-beräknad ET_a från FAO:s öppna databas WaPOR. En känslighetsanalys och en kalibrering med observerade flödesdata av SWAT-modellen utfördes med SUFI-2-algoritmen i SWAT-CUP. Kalibreringen var tillfredsställande och visade följande värden för prestandaparametrarna: R^2 = 0,72, Nash-Sutcliffe-Efficiency, NSE = 0,69 och Percent of Bias, PBIAS = -10,4. De mest känsliga parametrarna var CN2 (avrinningskurvtal för fukttillstånd II), SOL_AWC (jordens tillgängliga vattenkapacitet) och ESCO (kompensationsfaktor för markavdunstning). Vattenbalansfördelningen från den kalibrerade SWAT-modellen visade ett förhållande på 0,68 mellan ET_a och nederbörden som ett årligt medelvärde mellan 2012–2020.

I jämförelsen mellan SWAT ET_a och WaPOR ET_a visade SWAT ET_a en tydlig underskattning, särskilt under den torrare *Yala*-växtsäsongen (maj – augusti). Däremot överensstämde SWAT-markanvändningsklasserna som representerade de odlade risfälten väl med WaPOR medan skog och gräsfälten var underskattade. För att öka prestandan för SWAT vid uppskattning av ET_a rekommenderades följande: förbättring av simuleringen av de grunda akvifärerna, förbättrade skogsparametrar, inaktivering av den automatiska växtviloperioden i SWAT, kalibrering med ET_a i stället för flöde och en jordartskarta med högre upplösning samt fler jordprover.

Nyckelord: faktisk evapotranspiration, fjärranalys, Malwathu Oya, Sri Lanka, SWAT-modellering, SWAT-kalibrering, vattenbalans, WaPOR

Institutionen för Mark och Miljö, Sveriges Lantbruksuniversitet (SLU), Lennart Hjelms väg 9, SE 75007, Uppsala, Sverige. ISSN 1401-5765

Preface

This master's thesis covers 30 credits and concludes five years of studies at the programme of Environmental and Water Engineering at Uppsala University and Swedish University of Agricultural Sciences (SLU). The thesis has been done as a part of an internship at the International Water Management Institute (IWMI) in Colombo, Sri Lanka, and thanks to financial support by SIDA (Swedish International Development Agency) through a Minor Field Study (MFS) scholarship this project has been made possible. The thesis contributed to the KnoWat project (Knowing Water better: towards fairer and more sustainable access to natural resources), a project led by FAO (Food and Agriculture Organization of the United Nations) and conducted by IWMI together with the Irrigation Department of the Ministry of Mahaweli, and the Irrigation Department of Sri Lanka. KnoWat is funded by the German Federal Ministry of Food and Agriculture. The supervisor was Dr. Karthikeyan Matheswaran, regional researcher in water productivity at IWMI and the subject reader was Prf. Jennie Barron at the Department of Soil and Environment at SLU.

This thesis is twinned with the thesis "Evaluation of Crop Water Use and Rice Yield Using Remote Sensing and AquaCrop Model for Three Irrigation Schemes in Sri Lanka". The two theses are complementary, where this thesis focuses on water balance on a basin level and the other on irrigation scheme performance on a field level in the Malwathu Oya river basin, Sri Lanka.

I would like to direct a big thanks to my subject reader Prf. Jennie Barron for your support in the planning phase of this project and for your valuable inputs and interest in the project. I would also like to give a big thanks to Dr. Karthikeyan Matheswaran for your work in making this project possible and for your advice and support throughout the project. Thanks to IWMI for hosting me and giving me this opportunity, I felt very welcomed and learned a lot, and thank you to Dr. Lal Muthuwatta at IWMI for helping me with your expertise in the SWAT modelling and calibration.

I also want to thank Prf. Nimal Shantha Abeysingha and Dr. Nalaka Geekiyanage as well as students and staff at the Faculty of Agriculture, Rajarata University of Sri Lanka, for your help with the collection and analysing of field data and for your warm welcome.

At last, I want to thank my friend Veronika Widengren for being a great discussion partner and travel companion and thanks to my family and friends for your support during my studies.

Alexander Fors
Uppsala, June 2022

UPTEC W 22020, ISSN 1401-5765.
Digitally published at DiVA, 2022, through the Department of Earth Sciences, Uppsala University. (http://diva-portal.org/).

Populärvetenskaplig sammanfattning

I en tid med klimatförändringar och när människors behov av vatten för konsumtion och till jordbruk kan bli en bristvara är det viktigt med ett klokt användande av vattenresurser. För att kunna använda vatten mer resursklokt krävs beräkningar av vattenförbrukningen i landskapet och detta kräver mätdata, något som traditionellt samlats in via markobservationer. Mängden tillgängliga data från markobservationer är dock inte alltid tillräcklig och särskilt inte i utvecklingsområden. En av de viktigaste parametrarna vid beräkning av vattenförbrukning är den faktiska evapotranspirationen (ET_a). ET_a beskriver hur mycket vatten som tillförs atmosfären från avdunstning från jorden och från det vatten som växter transpirerar och det är därför viktigt med en bra uppskattning av ET_a för att räkna på nyttjandet av vattenresurser. Med hjälp av fjärranalys kan ET_a beräknas med en hög tidsupplösning utan någon inblandning av markobservationer och därmed underlätta beräkningen av användandet av vattenresurser i områden med låg datatillgänglighet. FN:s jordbruksorganisation FAO har därför utvecklat en dataportal som kallas WaPOR med fritt tillgängliga fjärranalysdata över bland annat ET_a.

I denna studie undersöktes hur väl ET_a från WaPOR stämmer överens med oberoende ET_a-data beräknad med den hydrologiska modellen SWAT för att undersöka tillförlitligheten hos WaPOR. SWAT-modellen kalibrerades med observerade flödesdata och en känslighetsanalys av dess parametrar gjordes även. Detta gjordes i avrinningsområdet Malwathu Oya i norra delen av Sri Lanka som ligger i landets torra zon och som därför är drabbat av torka under delar av året. En förbättrad förståelse av vattenresursanvändningen i området är därför viktig.

Kalibreringen med flödesdata som gjordes för SWAT-modellen var tillfredsställande enligt de prestandaparametrar som undersöktes och de mest känsliga parametrarna var de som styrde markens benägenhet för avrinning och de som hade med jordens vattenhållandeförmåga och avdunstning att göra. Ett årligt medelvärde på 1361 mm nederbörd och 922 mm ET_a beräknades i Malwathu Oya från SWAT-modellen. Från jämförelsen mellan WaPOR och SWAT ET_a visade SWAT mycket lägre värden, särskilt under den torrare växtsäsongen. Detta förklarades bland annat av brist på vatten i SWAT-modellen till följd av en icke-tillfredsställande simulering av vattnet i de grunda akvifärerna, andra orsaker var att växterna i SWAT automatiskt gick in i en viloperiod där de tappade en del av sin biomassa och därmed förmåga att transpirera och att en kalibrering med ET_a-data i stället för flöde troligtvis hade gett ett mer tillförlitligt resultat.

Table of Contents

List of Tables

List of Figures

Abbreviations

AWC	Available Water Capacity
DEM	Digital Elevation Model
ET	Evapotranspiration
ET_a	Actual Evapotranspiration
ET_o	Reference Evapotranspiration
ET_p	Potential Evapotranspiration
ETI_a	Actual Evapotranspiration and Interception
FAO	Food and Agriculture Organization of the United Nations
HI	Harvest Index
HRU	Hydrologic Response Unit
IWMI	International Water Management Institute
KnoWat	Knowing Water better: towards fairer and more sustainable access to natural resources (FAO project)
NDVI	Normalized Difference Vegetation Index
NIR	Near-Infrared
NSE	Nash-Sutcliffe Efficiency
PBIAS	Percent of Bias
P-M	Penman-Monteith
RS	Remote Sensing
SDG	Sustainable Development Goal
SLU	Swedish University of Agricultural Sciences
STD	Standard Deviation
SUFI-2	Sequential Uncertainty Fitting
SWAT	Soil and Water Assessment Tool
SWAT-CUP	SWAT Calibration Uncertainty Program
WaPOR	Water Productivity through Open access of Remotely sensed derived data
95PPU	95 Percent Prediction Uncertainty

1. Introduction

In a time where climate change is impacting people's access to water for domestic consumption and agricultural use (Pörtner et al. 2022) it is becoming more and more important to be able to monitor water use in an efficient way to battle water scarcity. To accomplish this data on various hydrometeorological parameters are needed which traditionally have been collected from ground observations, however, since the 1980s the amount of ground observations has been in a global decline (García et al. 2016). This is especially the case in developing regions where there is a scarcity of real-time ground observations due to a lack of accessibility, insufficient quality control, and availability (García et al. 2016). A tool that can be used as a solution for these problems is the use of satellite remote sensing. Satellite-based sensors can provide data of practically all components of the hydrological cycle, at a high temporal resolution and large spatial coverage, therefore facilitating water accounting and agricultural management (Sheffield et al. 2018). Actual evapotranspiration (ET_a) is one of the key parameters of the hydrological cycle and represents the water moving to the atmosphere from soil evaporation and plant transpiration (Brutsaert & York 2005). To assess the water balance in a watershed it is therefore important with a good estimate of this parameter.

The Malwathu Oya river basin in the North-Central province of Sri Lanka is the study area of this project. It is the country's second largest river basin and one of the major agricultural areas with rice as the dominant crop (Sivakumar et al. 2019; FAO n.d.a). The main sources of irrigation in the Malwathu Oya river basin are a large number of ancient rainfed reservoirs which sequentially drains into the river forming a tank cascade system (Geekiyanage & Pushpakumara 2013; Sivakumar et al. 2019; FAO n.d.a). It is located in the dry zone and because of this and climate change the river basin is prone to water scarcity at different times of the year, particularly in the *Yala* season (May – August) (FAO n.d.a). Therefore, the current management could be better informed by using high resolution data to improve the water use efficiency.

To address data scarcity on water and land productivity indicators in Sri Lanka, the Food and Agriculture Organization of the United Nations (FAO) has together with partners developed an open access database called WaPOR (Water Productivity through Open access of Remotely sensed derived data) which features various parameters for monitoring water productivity (FAO n.d.a). By using ET_a estimates from WaPOR it is possible to assess the water balance and to supplement hydrometeorological data. This can help support the United Nation's Sustainable Development Goals SDG 2, zero hunger, and SDG 6.4, water use and scarcity.

However, to increase the accuracy of remote sensed data there is a need to validate against independent data to ensure performance and reliability. Thus, to improve

the understanding of water balance in the Malwathu Oya river basin this study investigated how well remote sensing estimates of ET_a from WaPOR performed against ET_a obtained from the hydrological model SWAT (Soil and Water Assessment Tool) and the potential improvements of SWAT in estimating ET_a.

1.1. Aims and Objective

The objective of the thesis is to compare remote sensing estimates of actual evapotranspiration (ET_a) from the WaPOR database in the Malwathu Oya river basin with modelled ET_a from the hydrological model (SWAT) with the goal of improving the understanding of the river basin water balance and the accuracy of the remote sensing data. Potential improvements of the SWAT model in estimating ET_a are also investigated.

The project will combine literature studies and data collection in the Malwathu Oya river basin to support modelling approaches, and evaluation and validation of the WaPOR ET_a data.

1.2. Research Questions

- What is the water balance partitioning in the Malwathu Oya river basin based on a streamflow calibrated SWAT model?
- What SWAT parameters are sensitive to streamflow?
- How does remote sensing derived WaPOR ET_a compare to SWAT modelled ET_a?
- What are the potential improvements in the SWAT model for estimating ET_a?

2. Background

2.1. Remote Sensing

The use of remote sensing (RS) technology is now widely used as a tool for collecting hydro-meteorological data and can provide data over large spatial extent with high temporal resolution, thus facilitating the use of hydrological models compared to before when sufficient data was harder to acquire (Kumar & Reshmidevi 2013). The satellites used for remote sensing obtain data based on the radiation intensity of different portions of the electromagnetic spectrum. It is either by passive RS, the emission by the earth's surface from the sun (measured in the visible, near-infrared (NIR), thermal bands, or microwave bands), or from active RS, which measures the microwave radiation reflected by the surface from emission by the instrument (Kumar & Reshmidevi 2013; García et al. 2016). The passive RS sensors, also called optical RS when operating in the visible and NIR bands, are used for estimating parameters related to the vegetation and soil, such as land cover, Normalized Difference Vegetation Index (NDVI), and land surface temperature which can be used in the estimation of ET_a (van Dijk & Renzullo 2011). Nonetheless, a major limitation with optical RS techniques is the presence of cloud cover which it has a low capability of penetrating, thus leading to lower data quality. This is especially problematic in tropical regions where the cloud cover is frequent, like in Sri Lanka (Kumar & Reshmidevi 2013).

2.2. Evapotranspiration

Evapotranspiration (ET) is the combination of evaporation of water from the soil surface and transpiration by the crop. Evaporation is the process when liquid water is transforming into vapour while being removed from the surface of the liquid (Allen et al. 1998). For water to be evaporated energy is required and in nature direct solar radiation provides the majority of this energy whereas a minor part comes from the ambient air temperature (Allen et al. 1998). The difference in vapour pressure between the evaporating surface and the surrounding atmosphere is the driving force of this process and as the evaporation continues the surrounding air will start becoming saturated and evaporation will decrease or cease unless wind is transporting the saturated wet air to the atmosphere (Monteith & Unsworth 2013; Null et al. 2016). This process is strongly dependent on the speed of the wind and other important parameters related to the evaporation process are air humidity, air temperature, and solar radiation (Null et al. 2016).

Transpiration is the loss of water from vaporisation of liquid water within plant tissues to the atmosphere in the process of photosynthesis (Allen et al. 1998; Kirschbaum 2004). The plant loses most of the water by transpiration off the plant leaves as carbon dioxide needed for photosynthesis is absorbed from the atmosphere (Taiz & Zeiger 2002). The amount of water that is being transpired to the atmosphere is regulated by the aperture of the stomata which is varying with atmospheric water vapour pressure deficit, CO_2 concentration, leaf temperature, and leaf irradiance (Cowan 1978). Only a small fraction of the water that is taken up from the soil is used within the plant, the rest is lost by transpiration (Allen et al. 1998). There are many different parameters to consider when assessing transpiration. Transpiration shares the same parameters that affect evaporation, namely, wind speed, air humidity, air temperature, and solar radiation. Apart from those factors the rate of transpiration also depends on soil and crop properties like soil water content, soil conductivity of water to the roots, soil water salinity, and crop type (C_3 or C_4), to name a few (Cowan 1978; Allen et al. 1998; Munn 2002).

The ratio between evaporation and transpiration varies during the growing stage of the crop. In an early stage most of the water is lost through evaporation, but as the crop grows and develops a larger crop canopy, the ET ratio will be dominated by transpiration (Ventura et al. 2001).

2.2.1. Reference, Potential, and Actual Evapotranspiration

The reference evapotranspiration ET_o is defined as the evapotranspiration from a reference surface that is well watered (Allen et al. 1998). The reference surface is a hypothetical grass crop with predefined parameters such as albedo, crop height, and bulk surface resistance (Allen et al. 1998). ET_o is only affected by climatic parameters and is computed from weather measurements and solar radiation (FAO 2020a), crop characteristics and soil factors are not considered (Allen et al. 1998). It can for example be used as a reference that can be related to the ET of other surfaces, or to compare ET between different seasons and locations (Allen et al. 1998).

The potential evapotranspiration ET_p is referred to as “the possible rate of loss without any limits imposed by the supply of water” (Beven 2020). It is thus the evaporation that can occur when all soil and plant surfaces are wet, or the evaporation from a free water surface (Null et al. 2016). The actual evapotranspiration ET_a is defined by the amount that is actually evapotranspired and is limited by the water supply.

2.2.2. Penman-Monteith Equation

The Penman-Monteith (P-M) equation is the FAO's standard equation for calculating reference and actual evapotranspiration (FAO 2020a). It is a combination equation which combines the energy balance equation and the aerodynamic equation (FAO 2020a) and is expressed in Equation 1.

$$\lambda ET = \frac{\Delta(R_n - G) + \rho_a c_p \frac{(e_s - e_a)}{r_a}}{\Delta + \gamma(1 + \frac{r_s}{r_a})} \quad (1)$$

where:
λ = latent heat of evaporation [J kg^{-1}]
E = evaporation [kg m^{-2} s^{-1}]
T = transpiration [kg m^{-2} s^{-1}]
R_n = net radiation [W m^{-2}]
G = soil heat flux [W m^{-2}]
ρ_a = air density [kg m^{-3}]
c_p = specific heat of dry air [J kg^{-1} K^{-1}]
e_a = actual vapour pressure of the air [Pa]
e_s = saturated vapour pressure [Pa] which is a function of the air temperature
Δ = slope of saturation vapour pressure against the temperature curve [Pa K^{-1}]
Υ = psychrometric constant [Pa K^{-1}]
r_a = aerodynamic resistance [s m^{-1}]
r_s = bulk surface resistance [s m^{-1}]

These parameters are mainly measured or are calculated from weather data (Allen et al. 1998). The P-M equation is generally performing best of all methods for estimating reference evapotranspiration when considering diverse climates (Null et al. 2016) but the disadvantage is the large amount of data needed.

2.2.3. Hargreaves Method

The Hargreaves method only requires temperature data and extra-terrestrial radiation to calculate ET_p, thus making it a good method in data scarce regions. The method was developed using weighing lysimeters to calibrate the equation (Equation 2) (Hargreaves & Samani 1985). The limitation of the Hargreaves method is its performance under extreme weather conditions and it tends to overestimate ET_p in hot and humid conditions (as in Sri Lanka) (Trajkovic 2007; Gelcer et al. 2010; Sivaprakasam et al. 2011).

$$\lambda E_o = 0.0023 \times H_0 \times (T_{max} - T_{min})^{0.5} \times \left(\overline{T}_{av} + 17.8\right) \quad (2)$$

λ is the latent heat of vaporisation (MJ kg^{-1}), E_o is the potential evapotranspiration (mm d^{-1}), H_0 is the extra-terrestrial radiation (MJ m^{-2} d^{-1}), T_{max} is the maximum air temperature on a given day (°C), T_{min} is the minimum air temperature on a given day (°C), and $\overline{T}_{av}$ is the mean air temperature on a given day (°C).

2.2.4. Thornthwaite's Method

Thornthwaite's method (Thornthwaite 1948) is another way of estimating ET_p with temperature as the only climatic data input. The monthly ET_p is estimated after adjusting for variable daylight and length of the months (Willmott et al. 1985) and is shown in Equation 3. Thornthwaite's method estimates ET_p best in humid climates but with a substantial underestimation in drier climates (Jensen et al. 1990).

$$ET_p = 16 \times \left(\frac{10 \times T_{mean}}{J}\right)^{\alpha} \times \frac{N \times n}{365} \quad (3)$$

Where ET_p is the mean monthly potential evapotranspiration (mm/month), T_{mean} is the mean monthly temperature (°C), J is the annual heat index, α is the function of the annual heat index, N is the mean length of daylight of the days in the month (hours), and n is the number of days in the month.

2.3. WaPOR

The WaPOR database provides remotely sensed derived data over Africa, the Near East, and Sri Lanka, and on three different levels of spatial resolution: level 1 (250 m), level 2 (100 m), and level 3 (30 m) (FAO 2020a, n.d.a). The data component used in this study is ETI_a (actual evapotranspiration and interception) which has a temporal resolution of dekadal, monthly and annual values (FAO 2020a). The spatial resolution that will be used in this study is level 2 (100 m).

Interception is the process of rainfall being intercepted by the leaves of the plants, and then evaporated directly from their surface (FAO 2020a). The fraction of intercepted rain is relatively high when precipitation is low but decreases rapidly with increasing precipitation (FAO 2020a). Interception is determined by the vegetation cover (c_{veg}), leaf area index (LAI), and precipitation (P) and is expressed in Equation 4 (FAO 2020a):

$$I_{mm} = 0.2I_{LAI}\left(1 - \frac{1}{1 + \frac{c_{veg}P}{0.2I_{LAI}}}\right) \quad (4)$$

The E and T in WaPOR are calculated by using the ETLook model (Bastiaanssen et al. 2012) which is based on the FAO Penman-Monteith equation with an adaption for remote sensing input data (FAO 2020a). The data components WaPOR uses for calculating E, T, and I are shown in Figure 1.

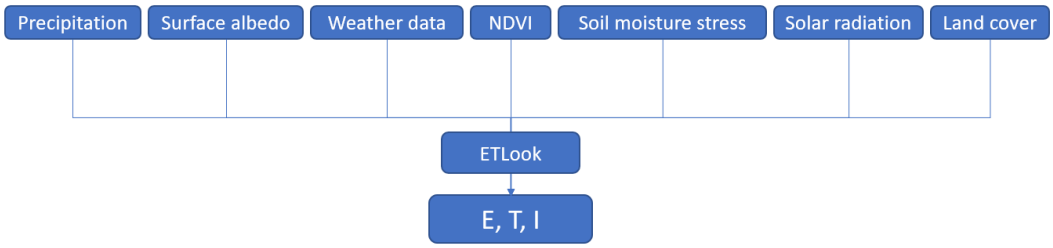

Figure 1: Data components used for calculating E, T, and I in WaPOR (FAO 2020a).

The E, T, and I are calculated on a dekadal basis and precipitation, weather data, and solar radiation are daily inputs, NDVI, soil moisture stress, and surface albedo are dekadal inputs and land cover is annual input (FAO 2020a).

The accuracy of WaPOR produced ETI_a is dependent on the presence of cloud cover in which case the optical satellite data such as NDVI cannot give information with a high temporal variability. When an area is covered by clouds WaPOR produces NDVI composites that fill gaps and missing data, and the accuracy of these composites get lower with a longer period of cloud cover (FAO 2020a).

Validation of WaPOR ETI_a products has previously been made in Africa and the Near East. In the WaPOR V2 quality assessment (FAO 2020b) it is found that there is a very high level consistency between level 1 and level 2 ETI_a data on a basin scale, and that for annual level 1 ETI_a data in Africa the fraction of ETI_a/P was >1 on 55% occasions for all basins between 2009-2018. ETI_a was also overestimated on average compared to the physical water balance on a basin scale. Moreover, Blatchford et al. (2020) found that WaPOR is overestimating ETI_a in dry and hot water-stressed conditions and in irrigated fields in Africa. No such studies have been performed in Sri Lanka however, so the same results are not necessarily the case in the climate there.

3. Materials and Methods

3.1. Site Description

Sri Lanka's topography consists of highlands in the south-central part of the country with an altitude of more than 2500 m, the other parts of the country are characterised by lowland plains (Geekiyanage & Pushpakumara 2013). Furthermore, Sri Lanka is divided into three climatic zones; a dry zone, a wet zone, and an intermediate zone (Muthuwatta et al. 2017). The dry zone lies in the north and eastern parts of the island and receives less than 1,750 mm of annual rainfall, the wet zone is in the south-western area and receives more than 2,500 mm of rainfall annually, and the intermediate zone lies between the two former zones and receives an intermediate amount of rain (Muthuwatta et al. 2017).

The yearly climate can be divided into four separate climate seasons, namely the first inter-monsoon from March to April, the south-west monsoon from May to September, the second inter-monsoon from October to November, and lastly the north-east monsoon from December to February (Muthuwatta et al. 2017). Moreover, the growing seasons are divided in two different periods; the *Maha* season, which is the major growing season across the whole country, and the *Yala* season which is the minor growing season of the dry zone (Muthuwatta et al. 2017). *Maha* begins in September and continues until March the following year and *Yala* begins in May and ends in August (Department of Census and Statistics n.d.).

The Malwathu Oya river basin is located in the dry zone and in the lowland plains. The location as well as the weather stations in the area can be seen in Figure 2. The size of the basin that is modelled in this study is 3,052 km^2 with elevation ranging from -10 to 721 m from the outlet in the northwest to the south. Rice is the main crop in the area (FAO n.d.a) and around 15% of the total basin area is used for paddy cultivation, for the most part during the *Maha* season (Muthuwatta et al. 2017). The irrigation in the dry zone is based on 7,620 ancient irrigation tanks, most of these are connected and form so called tank cascade systems, enabling water supply for the dry parts of the year (Panabokke et al. 2002).

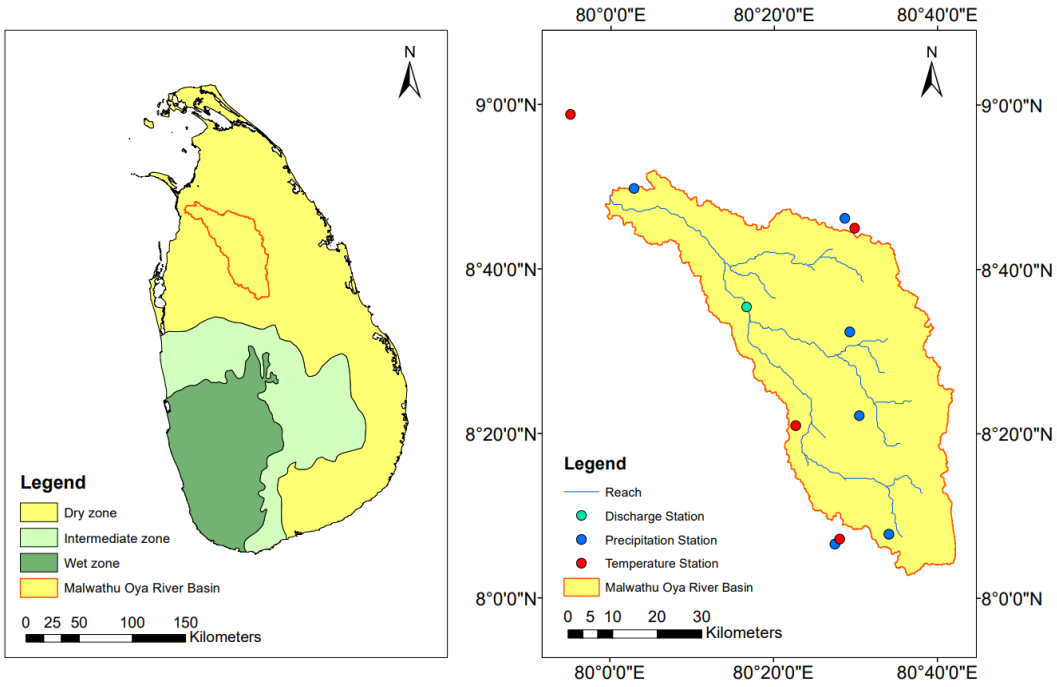

Figure 2: Location of the Malwathu Oya river basin in Sri Lanka with the three climate zones (Harischandra et al. 2016). The weather stations and discharge station in the river basin are also marked.

Figure 3 shows the mean monthly precipitation, ET_p, and T_{max} and T_{min} for the years 2010-2020 and their standard deviations based on daily precipitation and temperature data (Department of Meteorology Sri Lanka) from the weather stations seen in Figure 2. The mean annual precipitation between 2010 and 2020 is 1392 mm y^{-1}. The *Maha* season from September – March, received on average 1045 mm $season^{-1}$ and the *Yala* season from May – August, received on average 226 mm $season^{-1}$ between 2010 – 2020. The mean ET_p is 1828 mm y^{-1} and was calculated with Thornthwaite's method (Thornthwaite 1948). The mean monthly maximum temperature is 32 °C and the mean minimum temperature is 24 °C.

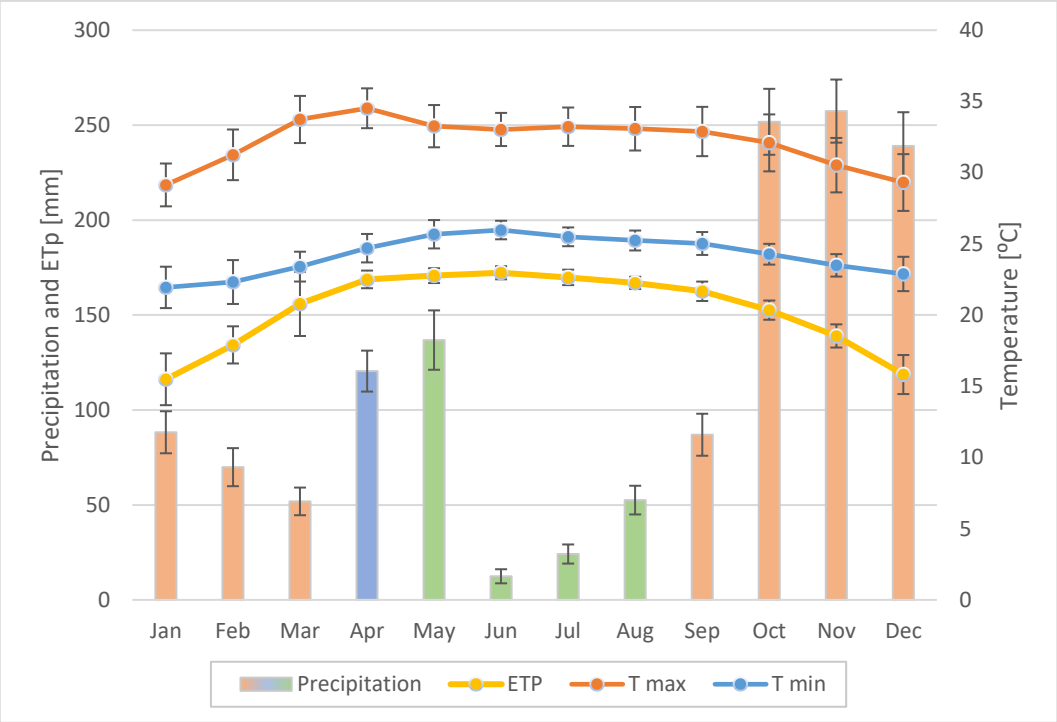

Figure 3: Monthly Average P (Maha season in orange bars and Yala in green), ET_p, T_{max} and T_{min} between 2010-2020 and their standard deviations. Calculated with daily data from weather stations (Department of Meteorology Sri Lanka) in and around the Malwathu Oya river basin.

3.2. Soil Sampling and Measurement of Infiltration Rate

Six soil samples were taken at 30 cm depth in Anuradhapura and were analysed for bulk density, texture, and Available Water Capacity (AWC) (which was derived from the texture). The samples were taken at three different locations with two samples at each site. Furthermore, the infiltration rate was determined at one location to derive the saturated hydraulic conductivity. For a detailed description of the methods used, see Appendix A. The location of where the soil samples were taken, and the measurement of infiltration rate was conducted can be seen in Figure 4. The figure also shows the soil map of the area which was used in the SWAT model with their different soil classes. The distribution and description of the different soils is shown in Table 1. The calculated bulk density, soil textures, AWC, and saturated hydraulic conductivity can be seen in Table 2.

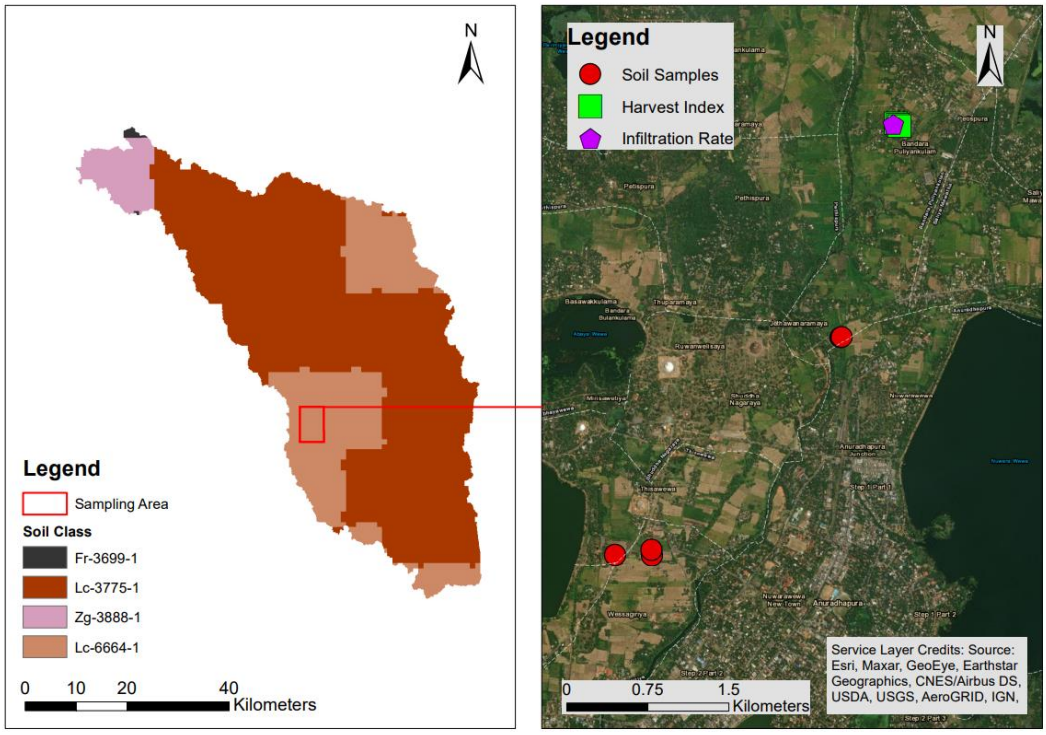

Figure 4: Soil map of Malwathu Oya river basin from NRMC, Sri Lanka, (https://doa.gov.lk/nrmc/) with the different soil classes and the area where the soil measurements and harvest index measurements were conducted.

Table 1: Description of the soil classes shown in the soil map. The soil classes are extracted from the Harmonized World Soil Database (HWSD), https://www.fao.org/soils-portal/data-hub/soil-maps-and-databases/harmonized-world-soil-database-v12/en/.

Soil Class	**Texture**	**Hydrologic Soil Group**	**Area (km^2)**
Fr-3699-1	Sandy clay loam	C	5.80
Lc-3775-1	Loam	C	2,157
Zg-3888-1	Loam	C	145.3
Lc-6664-1	Loam	C	744.1

Table 2: The measured soil parameters from the field samples.

Sample no.	**Bulk density (g cm^{-3})**	**Texture class**	**Sand %**	**Silt %**	**Clay %**	**AWC %**	**K_s (mm/hr)**
1	1.42	Sandy loam	84.4	2.3	13.3	5.8	104
2	1.27	Loamy sand	85.5	4.9	9.6	5.6	
3	1.31	Sandy loam	78.1	10.0	11.9	7.1	
4	1.67	Loamy sand	87.1	7.2	5.7	6.1	
5	1.77	Loamy sand	80.6	11.8	7.6	6.6	
6	1.61	Loamy sand	87.1	5.9	7.0	5.3	

Mean	1.50	Loamy sand	83.8	7.0	9.2	6.1	104

The mean measured soil texture class was loamy sand and the texture class of the soil in the sample area Lc-6664-1 is a loam. According to a study by (Rosemary et al. 2017) where 58 soil samples were taken in the alfisol catena of the dry zone in the first soil layer (0-30 cm), roughly 40 km southwest of this study's sample area, 61 % of the samples were sandy loam, 30 % loamy sand, and 9 % sandy clay loam.

3.3. Measurement of Harvest Index and Maximum Rooting Depth of Rice

The mean value of the harvest index (HI) of rice was calculated based on three measurements close to Anuradhapura, their location is shown in Figure 4. For a detailed description of the methods used to determine the Harvest index see Appendix A. The maximum rooting depth of the rice was calculated from the same three measurement sites as the harvest index by measuring the longest root of the rice plants of a total of 20 plants divided between the three locations and then calculating the mean value. The mean values were used as input in the SWAT model. The results from the measurements can be seen in Table 3.

Table 3: Mean, minimum (min), maximum (max), and standard deviation (SD) of the measured harvest index and maximum rooting depth of rice.

Variable	**Harvest index (HI)**	**Maximum rooting depth (m)**
Mean	0.324	0.11
Min	0.280	0.060
Max	0.350	0.14
SD	0.0316	0.020

3.4. Soil and Water Assessment Tool (SWAT)

The Soil and Water Assessment Tool (SWAT) with the ArcGIS extension ArcSWAT (version 2012.10_5.24) was used in this project to assess the water balance in the Malwathu Oya river basin and to validate the SWAT ET_a with WaPOR ET_a.

SWAT is a physically-based continuous time hydrological model with distributed landscape elements (so called Hydrologic Response Units, HRUs), that can be used

to simulate the water balance in a watershed over long time periods (Neitsch et al. 2011). The model has been applied in many different climatic zones and is one of the most used river basin-scale hydrological models worldwide (Gassman et al. 2014). The flexibility in SWAT to describe various environmental conditions and an open source code are some of the reasons behind its extensive use (Gassman et al. 2014).

To determine ET_a SWAT is first calculating $ET_{p,}$ which in this study is done with Hargreaves method. Next, the intercepted rainfall will be evaporated and thereafter a calculation of the maximum amount of transpiration and soil evaporation is made. The actual transpiration is then determined by the soil available water and the actual soil evaporation is determined by partitioning of the soil evaporative demand between the different soil layers (Neitsch et al. 2011).

There are several studies where SWAT has been applied in the dry zone of Sri Lanka. The Kala Oya river basin just south of this study's river basin Malwathu Oya was modelled with SWAT by (Iresh et al. 2021). The Kala Oya river basin is of similar size to Malwathu Oya and the streamflow for two gauging stations in the basin was simulated with a calibrated SWAT model with good simulated results for daily streamflow (Iresh et al. 2021). Furthermore, in a study by (Seenithamby & Nandalal 2021) SWAT was used to estimate the runoff/precipitation ratio in the Yan Oya river basin located near the Malwathu Oya river basin where the results showed a good linear relationship between runoff and precipitation.

3.4.1. Input Data

The SWAT input data that was used in this study to model the water balance was a Digital Elevation Model (DEM), land use map, climatic data, and a soil map with corresponding soil parameters. A full list of the input data can be seen in Table 4.

Table 4: Input data used for the SWAT model.

Data type	Data description	Source
DEM	90 x 90 m, HydroSHEDS Core Layers (version 1)	(Lehner et al. 2008) https://www.hydrosheds.org/
Land Use	10 x 10 m, ESA WorldCover 10 m 2020 V100.	(Zanaga et al. 2021)

Data type	Data description	Source
Climate	Climatic stations - daily precipitation and temperature (2010-2020)	Department of Meteorology Sri Lanka https://www.meteo.gov.lk/index.php?option=com_content&view=article&id=100&Itemid=321&lang=en
Vegetation	Rice parameters: harvest index, maximum rooting depth. Other crop and vegetation parameters.	Measured harvest index and maximum rooting depth. Crop and vegetation parameters from the SWAT land cover/plant growth database (Arnold et al. 2012).

Digital Elevation Model and Stream Network

To delineate the watershed the watershed delineation tool in ArcSWAT was used with the hydrologically conditioned DEM from HydroSHEDS (Lehner et al. 2008). The DEM was clipped to Malwathu Oya river basin by using a mask in the DEM setup in ArcSWAT and the streams were created based on the DEM and flow direction and accumulation. An outlet was manually added where the discharge station was located and the outlet for the whole river basin was selected, thereafter the watershed was delineated. A total of 26 subbasins were created based on the area of flow direction and accumulation which was 6100 Ha. A map of the DEM and the created stream network is shown in Figure 5.

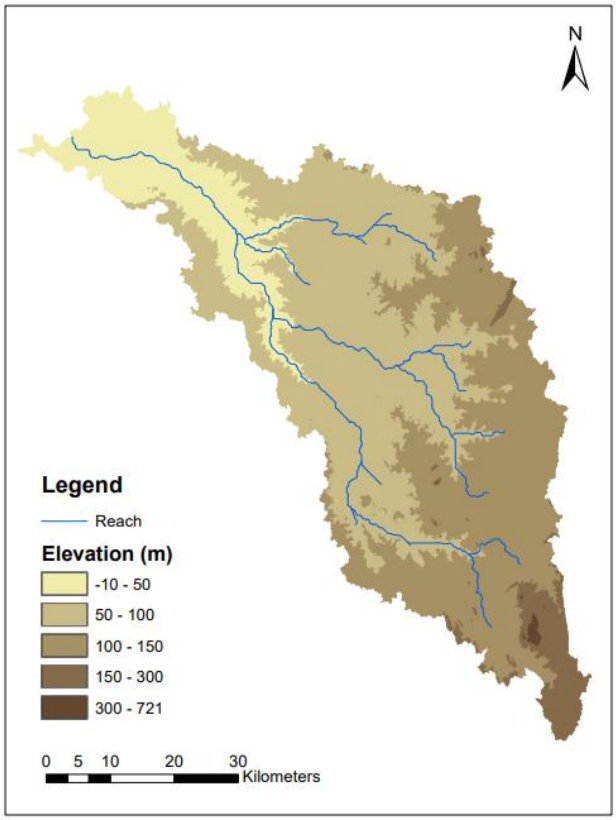

Figure 5: DEM over Malwathu Oya river basin with the stream network created in ArcSWAT (Lehner et al. 2008).

Land Use

The land use map used in this SWAT model was based on ESA WorldCover 10 m 2020 V100 (Zanaga et al. 2021). This map was reclassified manually in QGIS for agricultural lands with the help of Google Satellite imagery (Google, ©2022 CNES/Airbus, Landsat/Copernicus, Maxar Technologies) to improve the model performance. The reclassification was done by using the Google satellite imagery as a background of the land use map to detect agricultural lands that were not classified. The reclassification was done by using the Serval tool Plugin in QGIS by reclassifying the raster pixel values through manual selection and then assigning it to the agricultural land class. The ESA WorldCover 10 m agricultural land classification was thus improved through this process.

When finished, the land use map was classified according to the SWAT land use classes in ArcSWAT. The land use map can be seen in Figure 6 and in Table 5 the description of the land use classes and their area distribution are shown. A major part of the deciduous forest is located in the downstream area in the northwest as a part of the Wilpattu National Park.

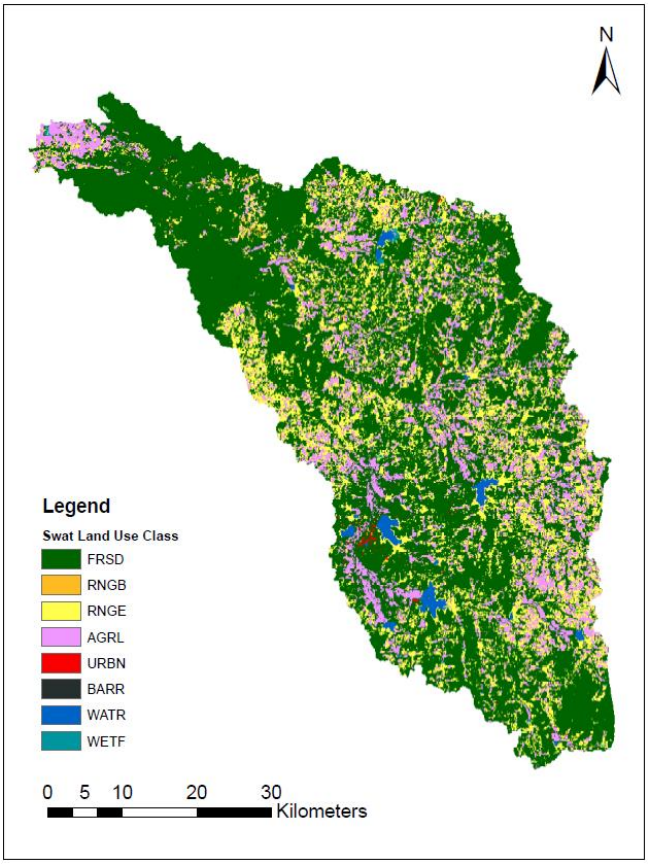

Figure 6: Land use map used in SWAT (© ESA WorldCover project 2020 / Contains modified Copernicus Sentinel data (2020) processed by ESA WorldCover consortium).

Table 5: Land use classification and description.

Land use classification	**SWAT land use class**	**Area (km^2)**	**Area of the basin (%)**
Forest-Deciduous	FRSD	1,943	63.7
Brush land	RNGB	6.95	0.23
Range-Grasses	RNGE	600	19.7
Agricultural	AGRL	444	14.5
Urban	URBN	6.36	0.21
Barren	BARR	10.6	0.35
Water	WATR	35.5	1.16
Wetlands-Forested	WETF	5.53	0.18

An example picture of agricultural land (rice field) is shown in Figure 7.

Figure 7: Picture of a rice field at the Rajarata University, Anuradhapura.

Climate

The climatic data that was used was from six rainfall gauges measuring precipitation and four temperature gauges measuring maximum and minimum temperature. Their spatial distribution is shown in Figure 2. Both data sets were daily from 2010-2020 and was provided by the Department of Meteorology in Sri Lanka. There were less than 10% of missing data and where data was missing it was generated by using a linear regression equation by correlating the data with nearby stations (Longman et al. 2020), this was done by the Department of Meteorology in Sri Lanka. Table 6 shows the coordinates and names of the climatic stations and the type of data.

Table 6: Climate data and its sources used in the SWAT model.

Climate station	**Coordinates (lat., long.)**	**Data from 2010-2020 (daily)**
Mahailluppallama	8.11, 80.46	Precipitation
Maradankadawala	8.13, 80.57	Precipitation
Medawachchiya	8.54, 80.49	Precipitation
Mihintale	8.37, 80.51	Precipitation
Murunkan	8.83, 80.05	Precipitation
Vavuniya	8.77, 80.48	Precipitation
Mannar	8.98, 79.92	Temperature

Vavuniya	8.75, 80.50	Temperature
Mahailluppallama	8.12, 80.47	Temperature
Anuradhapura	8.35, 80.38	Temperature

Soil

The soil map that was used was from the Natural Resources Management Centre of the Department of Agriculture (NRMC), Sri Lanka (https://doa.gov.lk/nrmc/). The original scale was 1:500,000 but the map has been digitized and resampled into 100 x 100 m pixels. Soil parameters for the first two layers of each soil class were extracted from the Harmonized World Soil Database (HWSD), (https://www.fao.org/soils-portal/data-hub/soil-maps-and-databases/harmonized-world-soil-database-v12/en/) and were inserted in the SWAT2012 database in the usersoil tab. The mean values of the measured soil parameters from the field (see Table 2) were inserted in the first soil layer for the soil type in which they were measured (Lc-6664-1). The soil parameters for the two layers are described in Table 7 and the values used in the SWAT model are shown in Table 8.

Table 7: Description of soil parameters used in SWAT and their units (Arnold et al. 2012).

SWAT name	**Description**	**Unit**
SOL_ZMX	Maximum rooting depth of soil profile	mm
ANION_EXCL	Fraction of porosity from which anions are excluded	-
SOL_CRK	Potential or maximum crack volume as a fraction of the total volume	-
SOL_Z(layer#)	Depth from soil surface to bottom of layer	mm
SOL_BD(layer#)	Bulk density	g cm^{-3}
SOL_AWC(layer#)	Available water capacity	mm H2O/mm soil
SOL_K(layer#)	Saturated hydraulic conductivity	mm hr^{-1}
SOL_CBN(layer#)	Organic carbon content	% soil weight
CLAY(layer#)	Clay content	% soil weight

SILT(layer#)	Silt content	% soil weight
SAND(layer#)	Sand content	% soil weight
ROCK(layer#)	Rock fragment content	% total weight
SOL_ALB(layer#)	Moist soil albedo	-
USLE_K(layer#)	USLE soil erodibility (K) factor	0.013(metric ton m^2h)/(m^3-metric ton cm)

Table 8: The soil parameters for the two soil layers of each soil class that were used in the SWAT model. The soil parameters were extracted from the Harmonized World Soil Database (HWSD). The mean values of the measured soil parameters (Table 2) were inserted in the Lc-6664-1 soil class.

Soil class / **Parameter**	**Fr-3699-1**	**Lc-3775-1**	**Zg-3888-1**	**Lc-6664-1**
SOL_ZMX	1000	1000	1000	1000
ANION_EXCL	0.5	0.5	0.5	0.5
SOL_CRK	0.5	0.5	0.5	0.5
SOL_Z1	300	300	300	300
SOL_BD1	1.38	1.34	1.40	1.50
SOL_AWC1	0.11	0.14	0.16	0.061
SOL_K1	25.54	13.24	8.75	104
SOL_CBN1	0.68	0.86	0.42	0.86
CLAY1	26	24	21	9.2
SILT1	12	29	43	7.0
SAND1	62	47	36	83.8
ROCK1	3	9	6	9
SOL_ALB1	0.22	0.22	0.22	0.22
USLE_K1	0.12	0.13	0.16	0.13
SOL_Z2	1000	1000	1000	1000
SOL_BD2	1.36	1.35	1.35	1.35
SOL_AWC2	0.07	0.14	0.14	0.14
SOL_K2	149.24	7.67	7.67	7.67
SOL_CBN2	0.03	0.03	0.03	0.03
CLAY2	8	28	28	28
SILT2	1	29	29	29
SAND2	91	43	43	43
ROCK2	30	1	1	1
SOL_ALB2	0.26	0.22	0.22	0.22
USLE_K2	0.05	0.16	0.16	0.16

Vegetation
To describe the rice, parameters from the SWAT land use/crop data base (Arnold et al. 2012) and the measured harvest index and maximum rooting depth were used. For a full list of the rice parameters used in the model, see Appendix B. The rice was also modelled according to the *Maha* and *Yala* season every year by changing the management practices (see section 3.5). The other vegetation classes were not altered due to time constraint and the default parameters from the SWAT land use/crop data base were used.

3.5. SWAT Model Setup

To set up the SWAT model with all the input data the ArcSWAT toolbar in ArcGIS was used. The steps of setting up the model in ArcSWAT follows below.

Watershed Delineation
Here the watershed was delineated using the DEM as described in section 3.4.1.

HRU Analysis
In SWAT, Hydrologic Response Units or HRUs are land areas within each subbasin that consists of unique combinations of land use, soil and slope classes (Neitsch et al. 2011). The HRUs add accuracy to the simulation by improving the prediction of loadings from the subbasins, and as a general rule, a subbasin should consist of 1-10 HRUs (Arnold et al. 2012).

To begin setting up the HRUs the Land use/Soils/Slope Definition tab under HRU analysis was defined. In the land use tab, the land use map was chosen, and it was assigned the SWAT land use classes shown in Table 5. To represent the paddy fields, the land use class of the agricultural lands, AGRL, was changed to the SWAT land use class RICE. The RICE land use class contains crop parameters on rice from the SWAT plant growth database (Arnold et al. 2012). Since about 15 % of the land use in Malwathu Oya is paddy fields (Muthuwatta et al. 2017) and the area of agricultural lands, AGRL, in Table 5 also makes up about 15 % of the land use (14.5 %), all agricultural lands were assumed to be paddy. Next, in the soil tab, the soil map was selected, and the soil classes were added. Lastly the slope classes for the river basin were defined. In this case 4 slope classes were created from 0-2 %, 2-3 %, 3-5 %, and >5 %. This was based on the slope data in the basin with mean slope of 1.86 %, minimum slope of 0 %, maximum 91.1 % and standard deviation 3.35 %. When this was finished, an HRU feature class and an overlay report were created where the distribution of land use, soil, and slope classes in the basin were described.

When the land use, soils, and slope had been defined the definition of the HRUs was determined. Multiple HRUs were created based on a land use threshold of 10 % (land use over subbasin area), 15 % soil class over land use area and 10 % slope class over soil area. The thresholds were chosen to create around 10 or less HRUs per subbasin. In total 207 HRUs were created in the 26 subbasins.

Write Input Tables
Here the precipitation and temperature files were selected. Afterwards, all the SWAT input tables were created.

Edit SWAT Input
Here the parameters of RICE were edited in the SWAT land cover/plant growth database by changing the harvest index to the measured value of 0.324 and the maximum root depth to the measured value of 0.11 m. Furthermore, the management operations were edited for all HRUs containing the RICE land cover. This was done by applying the management operations "Planting/beginning of growing season" and "Harvest and kill" for the *Maha* season (September – March) and *Yala* season (May – August) for all 11 years that were simulated.

The auto irrigation and auto fertilization operations were also added for all RICE HRUs in the management operations. For the auto irrigation it was chosen to let the irrigation be triggered by the plant water demand. This was controlled by the water stress threshold which is the ratio of actual to potential plant transpiration and it is normally set between 0.90-0.95 (Arnold et al. 2012), in this study 0.95 was used. Thus, when the plant is water stressed the model adds water until the soil reaches field capacity. Other parameters related to the auto irrigation were; the irrigation efficiency, set to 57 % (based on calculations from (Brouwer et al. 1989)), the amount of water applied each time the irrigation is triggered, set to 75 mm (Department of Agriculture Sri Lanka 2021), and the source of irrigation which was set to an unlimited water source outside the watershed.

The auto fertilization used elemental nitrogen which was triggered by a nitrogen stress threshold, in this study set to 0.95 (Arnold et al. 2012). The other parameters used the default auto fertilization values.

SWAT Simulation
The SWAT model was run on a daily timestep for 11 years between 2010-2020 with a 2-year warm-up period during which no output results were printed. The output was selected to be printed on a monthly time step. After this a sensitivity

analysis and a calibration based on streamflow was performed which are described in the next two subchapters.

3.6. Sensitivity Analysis

A global sensitivity analysis was performed using the SWAT-CUP program (version 5.1.6.2). SWAT-CUP is a semi-automatic calibration program developed for SWAT (Abbaspour 2015) and provides several methods for calibration of SWAT models as well as sensitivity analysis.

The global sensitivity analysis estimates the sensitivity of each parameter from the average change in the objective function that results from changes in each parameter, while all other parameters are changing (Abbaspour 2015). The t-stat and p-value are the indicators which determine the degree of sensitivity. The t-stat value is the coefficient of the parameter divided by its standard error and the larger the absolute t-stat value, the more sensitive is the parameter. The p-value determines the significance of the sensitivity by testing the null hypothesis that the coefficient of the parameter is equal to zero - meaning it has no effect, and a p-value < 0.05 is generally accepted as the point where one can reject the null hypothesis, thus regarding the parameter as sensitive (Abbaspour 2015).

In this study the SWAT model was calibrated against observed discharge data and the sensitivity analysis was performed to eliminate the less sensitive parameters from the calibration process. The parameters that were chosen for this study were based on previous studies that considered calibration against discharge data (Abbaspour et al. 2007; J. G. Arnold et al. 2012; Iresh et al. 2021). The chosen parameters and their initial value ranges are presented in Appendix C. The sensitivity analysis was performed using the Sequential Uncertainty Fitting (SUFI-2) (described more in section 3.7) method by running one iteration with 500 simulations and then eliminating the parameters with a p-value > 0.10 before continuing the calibration with further iterations. A p-value > 0.10 was chosen to include more parameters in the calibration.

3.7. SWAT Calibration

The SWAT model was calibrated with monthly average observed discharge data provided by the Irrigation Department in Sri Lanka from the station shown in Figure 2 which is in Thanthirimale (Lat. 8.59, Long. 80.28). The model was calibrated between January 2012 – September 2020 (excluding the two warm up years 2010 and 2011 in SWAT). The average discharge data for three months were missing.

The observed discharge data that was used in the calibration is shown in Appendix C.

The calibration was performed with SWAT-CUP (version 5.1.6.2), and in this study the Sequential Uncertainty Fitting (SUFI-2) method was used. The SUFI-2 algorithm is calibrating the model based on parameters and parameter value ranges chosen by the user with the goal of finding the best range for each parameter (Abbaspour et al. 2004). The best ranges of the simulation are evaluated by the p-factor and r-factor. The p-factor represents the amount of measured data that is covered by the 95 Percent Prediction Uncertainty (95PPU) and the r-factor represents the thickness of the 95PPU i.e., the average distance between the 97.5 and the 2.5 percentiles (Abbaspour et al. 2007). The p-factor ranges from 0 to 1, where 1 means that 100% of the measured data is bracketed by the 95PPU. The r-factor is desired to be less than 1 and an r-factor of 0 and a p-factor of 1 means that the simulation exactly matches the measured data (Abbaspour et al. 2007).

Further, the performance of the model was evaluated by the coefficient of determination (R^2), Nash-Sutcliffe efficiency (NSE), and percent of bias (PBIAS) shown in equations 5, 6, 7. The chosen objective function of the model was NSE.

$$R^2 = \frac{\left[\sum_{i=0}^{n}(Q_{m,i} - \overline{Q}_m)(Q_{s,i} - \overline{Q}_s)\right]^2}{\sum_{i=0}^{n}(Q_{m,i} - \overline{Q}_m)^2 \sum_{i=0}^{n}(Q_{s,i} - \overline{Q}_s)^2} \quad (5)$$

$$NSE = 1 - \frac{\sum_{i=0}^{n}(Q_{m,i} - Q_s)^2}{\sum_{i=0}^{n}(Q_{m,i} - \overline{Q}_m)^2} \quad (6)$$

$$PBIAS = 100 \times \frac{\sum_{i=0}^{n}(Q_m - Q_s)_i}{\sum_{i=0}^{n} Q_{m,i}} \quad (7)$$

In above equations Q represents the discharge, m stands for measured value, s for simulated value, $\overline{Q}_m$ and $\overline{Q}_s$ are the means of the measured and simulated data, and n is the number of observations. The calibration can be seen as satisfactory if $R^2 > 0.5$, NSE > 0.5, and PBIAS < ±25 (Moriasi et al. 2007).

The calibration was run with 500 simulations in each iteration for a total of 3 iterations. The parameter values were changed either by replacing the existing value with a given value or by multiplying the existing value by (1 + a given value). The parameters that were calibrated can be seen in Appendix C. After each iteration the new parameter ranges that were provided by SWAT-CUP were checked so that they were in physically meaningful ranges.

When the calibration was finished, the parameters from the best simulation in the last iteration were exported and replaced the previous parameter values in the SWAT model.

3.8. Water Balance Components

The water balance in SWAT is based on Equation 8 (Neitsch et al. 2011):

$$SW_t = SW_0 + \sum_{i=1}^{t}(R_{day} - Q_{surf} - E_a - w_{seep} - Q_{gw}) \qquad (8)$$

where SW_t denotes the final soil water content (mm), SW_0 denotes the initial soil water content (mm), t is the time in days, R_{day} is the precipitation on day i (mm), Q_{surf} is the surface runoff on day i (mm), E_a is the actual evapotranspiration (mm), w_{seep} is the amount of water entering the vadose zone (mm), and Q_{gw} is the return flow (mm).

The water balance for the simulated period between 2012-2020 was analysed by assessing the average annual basin values which were derived from the SWAT output.std file.

3.9. Comparison of SWAT ET_a with WaPOR ET_a

To compare the SWAT ET_a with WaPOR ET_a the WaPOR ET_a data had to be prepared. First, level II (100 m resolution) monthly ET_a WaPOR data over Sri Lanka was downloaded from the WaPOR portal[1] for the period 2015-2020. The SWAT model was calibrated and run for the years 2012-2020 but the first year of available WaPOR data is from 2015. Next the WaPOR data was clipped to the SWAT modelled area of the Malwathu Oya river basin, and the mean value and standard deviation of the monthly rasters were calculated.

The monthly mean values and standard deviations from WaPOR were aggregated to a seasonal value for the *Maha* and *Yala* seasons, September – March and May – August, respectively. The same seasonal aggregation was done with the SWAT monthly calculated ET_a values for the river basin and the two datasets were compared. SWAT ET_a was thus represented as a point value for the whole river basin and WaPOR as a mean value of all the pixels in the river basin. The average

[1] https://wapor.apps.fao.org/catalog/WAPOR_2/2/L2_AETI_M

precipitation for the *Maha* and *Yala* seasons based on the weather stations in the river basin and the ET_p calculated from the SWAT model with Hargreaves method were also compared with the SWAT and WaPOR ET_a.

Comparison Based on Land Use Class

To perform a comparison based on the land use classes the SWAT annual ET_a output from all the HRUs (207) was extracted from the HRU output file. The HRUs containing the same land use class were grouped together to obtain the ET_a data from 2015-2020 based on the different land use classes. In order to compare the annual HRU ET_a with WaPOR ET_a, WaPOR annual ET_a (100 m resolution) from 2015-2020 was first downloaded from the WaPOR portal. Next, to represent WaPOR ET_a with the same amount of datapoints as the HRUs, the WaPOR data cells were aggregated with the Aggregate Tool (Spatial Analyst) in ArcGIS. The aggregation technique that was chosen was "mean", thus, the mean value of the input cells was used for the new aggregated cell. The assigned cell factor was 39, thereby increasing the original cell size by a factor of 39. This resulted in an aggregated raster with 212 cells. This was the closest number to the 207 HRUs that could be achieved. Thereafter, the Int Tool (Spatial Analyst) in ArcGIS was used to convert the raster values to integers in order to be able to export the raster values from the attribute tables. Lastly, the ET_a of the HRUs with the same land use class were compared to the 212 WaPOR ET_a cells by creating boxplots with the annual ET_a data from 2015-2020.

4. Results

4.1. Sensitivity Analysis

The results of the global sensitivity analysis are shown in Table 9 where the parameters are ranked from highest to lowest sensitivity. The runoff curve number CN2 showed the highest sensitivity followed by SOL_AWC, the soil available water capacity in layer 1, and ESCO, the soil evaporation compensation factor. Considering the t-stat value CN2 was notably more sensitive than SOL_AWC and ESCO with a t-stat value of -25.114 compared to 5.375 and -5.088, respectively. The least sensitive parameter was ALPHA_BF, the baseflow alpha factor, followed by SOL_K, the soil saturated hydraulic conductivity in layer 1, and CH_N2, Manning's "n" value for the main channel. Only the first 7 parameters were used for the calibration since they had a p-value < 0.10.

Table 9: The calibration parameters ordered after highest to lowest global sensitivity. See Appendix C, Table C2 for a description of the parameters.

Input parameter	t-stat	P-value	Ranking
r__CN2.mgt	-25.114	0.000	1
r__SOL_AWC(1).sol	5.375	0.000	2
v__ESCO.hru	-5.088	0.000	3
v__ALPHA_BNK.rte	-4.959	0.000	4
v__GW_REVAP.gw	3.000	0.003	5
v__CH_K2.rte	2.097	0.036	6
r__HRU_SLP.hru	1.635	0.098	7
v__GWQMN.gw	1.543	0.124	8
v__REVAPMN.gw	-1.488	0.137	9
v__SURLAG.bsn	1.371	0.171	10
r__SLSUBBSN.hru	1.250	0.212	11
v__GW_DELAY.gw	-1.195	0.233	12
r__EPCO.bsn	0.819	0.413	13
r__SOL_BD.sol	0.794	0.428	14
r__OV_N.hru	-0.516	0.606	15
v__CH_N2.rte	0.383	0.702	16
r__SOL_K(1).sol	-0.369	0.712	17
v__ALPHA_BF.gw	-0.184	0.854	18

4.2. SWAT Calibration

The calibrated parameters, their descriptions, and their final values/minimum and maximum ranges after the last iteration are shown in Table 10. The value range for CN2 was between 71 – 85 which according to the land use and hydrologic soil groups are reasonable values (Soil Conservation Service Engineering Division 1986). The GW_REVAP parameter which in SWAT refers to water moving from the shallow aquifer to the root zone had a value of 0.11, the value should be between 0.02 – 0.2 (Arnold et al. 2012), thus indicating a medium rate of transfer from the shallow aquifer to the root zone. The SOL_AWC in layer 1 had a value range from 0.12 – 0.31 (mm H_2O/mm soil). These values are very high compared to a soil study in the dry zone by Mapa & Pathmarajah (1995) where values in the range of 0.083 – 0.12 (mm H_2O/mm soil) were found. The ESCO parameter had a value of 0.17 where the possible range is from 0.01 – 1, a low value indicates that the model can extract water from deeper soil levels to meet the soil evaporative demand. The CH_K2 had a value of 67 (mm/hr) indicating a high loss rate of water (Arnold et al. 2012). The ALPHA_BNK value of 0.19 means that there is a steep recession curve for bank flow (Arnold et al. 2012). Lastly the HRU_SLP had a range of 0.001 – 0.252 (m/m) which is reasonable since the elevation in the river basin mostly is flat with a few hills.

Table 10: SWAT parameters that were calibrated and their final value / ranges after calibration in SWAT-CUP. The "r" before the parameter means a relative change was applied by multiplying the existing value by (1 + calibrated value). The "v" before the parameter means that the existing value was replaced by the calibrated value. For the calibrated values of the parameters with a relative change see Appendix C.

Input parameter	**Description** (Arnold et al. 2012)	**Final value / min and max range**
r__CN2.mgt	Initial Soil Conservation Service (SCS) runoff curve number for moisture condition II	71 – 85
v__GW_REVAP.gw	Groundwater "revap" coefficient	0.11
r__SOL_AWC(1).sol	Available water capacity of the soil layer (1) (mm H_2O/mm soil)	0.12 – 0.31
v__ESCO.hru	Soil evaporation compensation factor	0.17
v__CH_K2.rte	Effective hydraulic conductivity in main channel alluvium (mm/hr)	67
v__ALPHA_BNK.rte	Baseflow alpha factor for bank storage (days)	0.19
r__HRU_SLP.hru	Average slope steepness (m/m)	0.001 – 0.252

The 95PPU created from the last iteration is shown in Figure 8. The best simulation matches the observed discharge well for the most part. The simulated baseflow is generally slightly higher than the observed and the small rainfall peaks are exaggerated in the simulation. For some of the bigger discharge peaks the simulated discharge is under predicting, especially at the biggest peak in November 2015. In October 2012 a double peak is shown for the simulation where the first peak is likely caused by a local rainfall event not affecting the streamflow much. The simulated peak at the end of 2014/beginning of 2015 is showing a long lag time and for the peak at the end of 2018/beginning of 2019 the simulated curve has a shorter lag time than the observed peak.

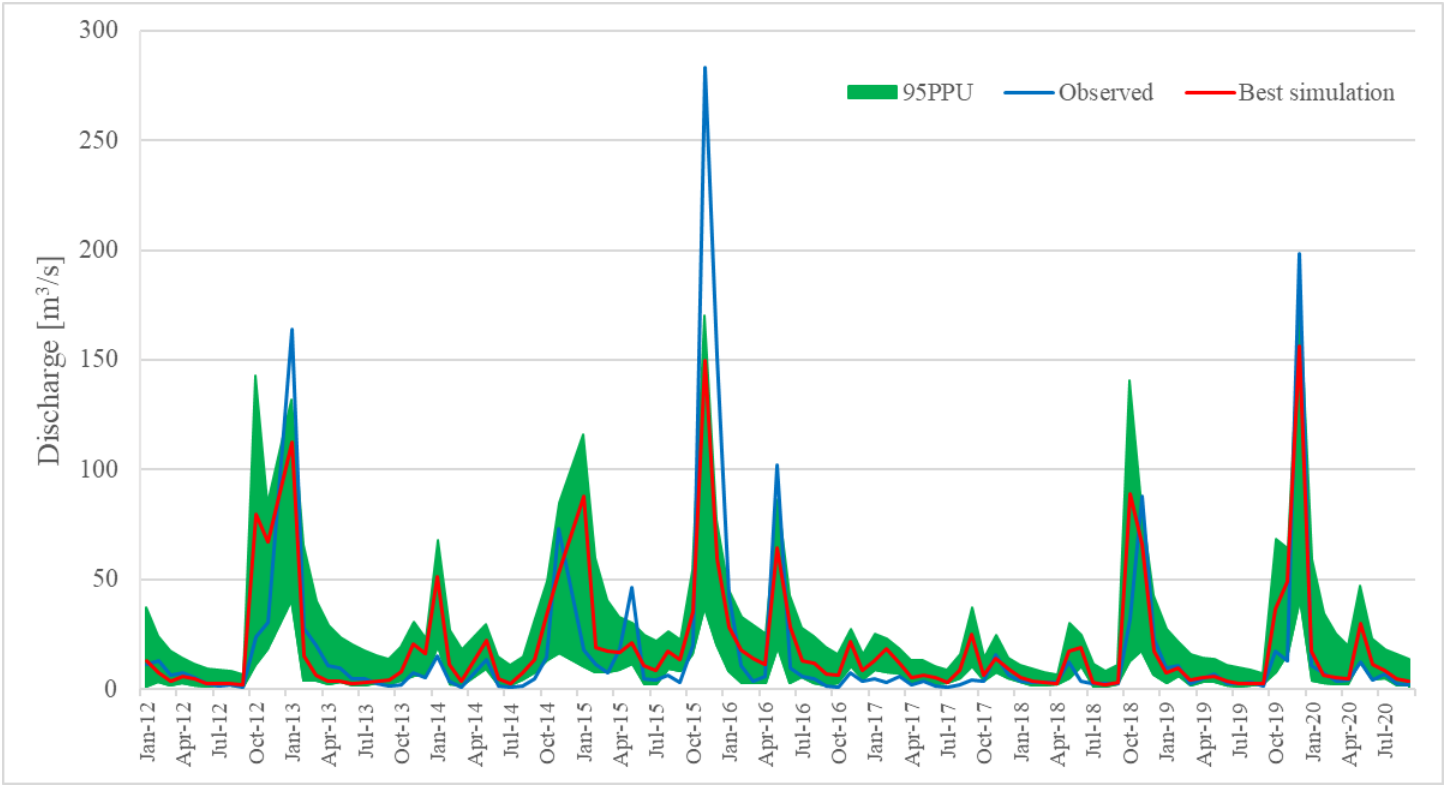

Figure 8: The 95PPU graph with the best simulation from the last iteration.

According to the evaluation coefficients used in the calibration the results are satisfactory (Moriasi et al. 2007) with an R^2 value of 0.72, NSE 0.69, and PBIAS -10.4. The p-factor from the 95PPU was 0.66 and the r-factor 0.68. A summary of the calibration statistics is presented in Table 11.

Table 11: Summary statistics from the calibration.

p-factor	**r-factor**	**R^2**	**NSE**	**PBIAS**
0.66	0.68	0.72	0.69	-10.4

4.3. Water Balance Components

The water balance results from the SWAT simulation show that the average annual precipitation between 2012-2020 was 1361 mm and the average ET_a was 922 mm, or 68 % of the precipitation. Moreover, the baseflow (shallow aquifer flow + lateral soil flow) was 18 % of the total flow and the surface runoff was 19 % of the precipitation. The total water yield was 338 mm, i.e., the sum of surface runoff, lateral soil flow, and shallow and deep aquifer flow. A visual representation of the water balance in the Malwathu Oya river basin is shown in Figure 9. Since the water balance equation in SWAT includes the initial soil water content the sum of the evapotranspiration, water yield, and aquifer recharge exceeds the precipitation.

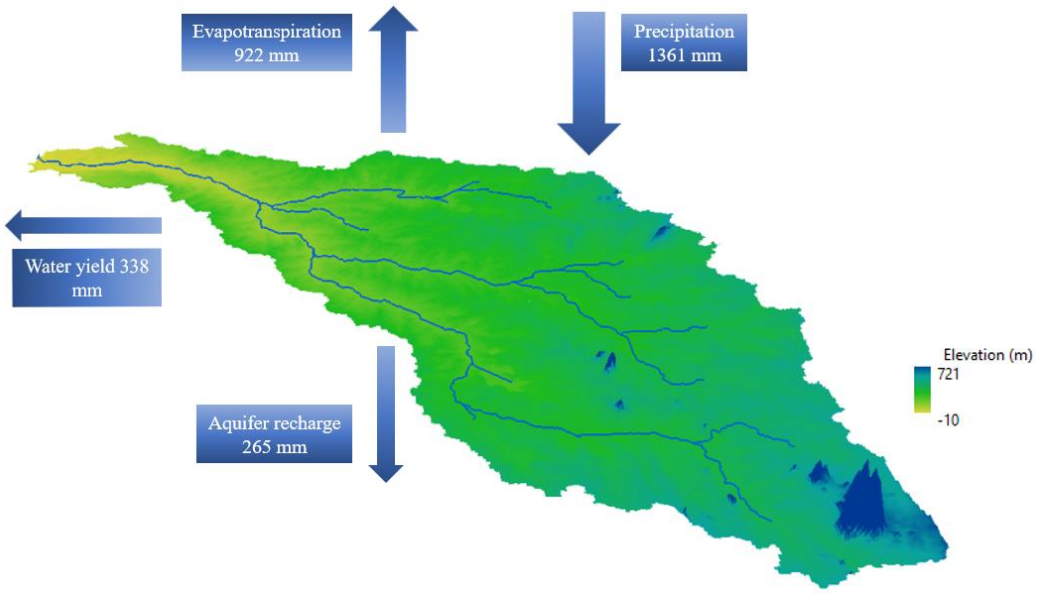

Figure 9: Visual representation (not to scale) of the water balance in the Malwathu Oya river basin with the main water balance components showing the annual average values between 2012-2020.

A complete list of the average annual water balance components between 2012-2020 is shown in Table 12.

Table 12: The SWAT average annual water balance values for the Malwathu Oya river basin between 2012-2020.

Component	Average annual value (mm/year)	Standard deviation (mm/year)
Precipitation	1361	330
Surface runoff	264	147
Lateral soil flow	7	1.1
Shallow aquifer flow	54	41
Deep aquifer flow	13	8
Revap (shallow aquifer to soil/plants)	177	17
Deep aquifer recharge	13	7
Total aquifer recharge	265	200
Total water yield	338	143
ET_a	922	108

4.4. Comparison of SWAT ET_a with WaPOR ET_a

The aggregated monthly values of SWAT ET_a and WaPOR ET_a for the *Maha* and *Yala* seasons (September-March and May-August, respectively) from 2015-2020 in the Malwathu Oya river basin and the average precipitation are shown in Figure 10. The overall conclusion from the graph is that SWAT ET_a shows much lower values compared to the WaPOR ET_a. The difference is biggest in the *Yala* seasons, while SWAT ET_a is the same as WaPOR in *Maha* 15/16. The last three *Maha* seasons show an underprediction by SWAT by around 100 mm/season and the most similar *Yala* season is *Yala 2020* with about a 100 mm lower SWAT value. Based on the precipitation data SWAT shows very low ET_a values during the *Yala* season when the precipitation is low and values closer to WaPOR during the *Maha* season when the precipitation is higher. The WaPOR data shows a similar pattern between the seasons although with higher ET_a values that exceed the precipitation on several seasons.

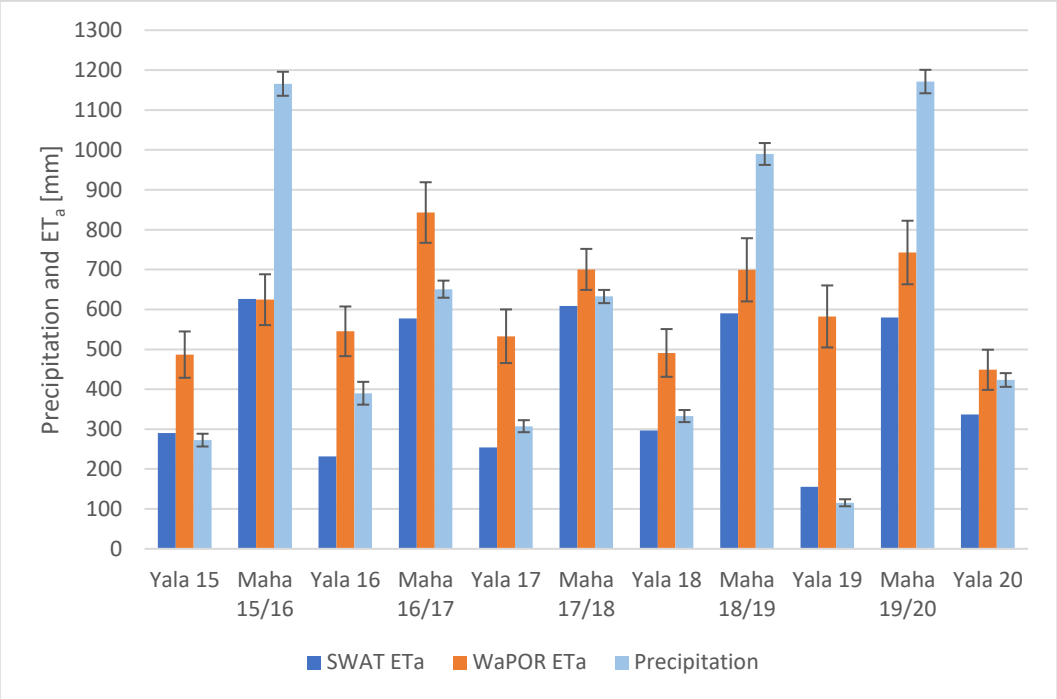

Figure 10: SWAT ET_a, WaPOR ET_a and precipitation for the Maha and Yala seasons from 2015-2020. The WaPOR ET_a and precipitation are shown with standard deviation. The precipitation represents the average precipitation from the climatic stations.

The SWAT and WaPOR ET_a were also compared with ET_p Hargreaves during the same period and seasons, this is shown in Figure 11. The WaPOR ET_a is showing similar values to the ET_p in the *Yala* season with approximately 10 – 100 mm/season less, whereas the differences are bigger in the *Maha* season.

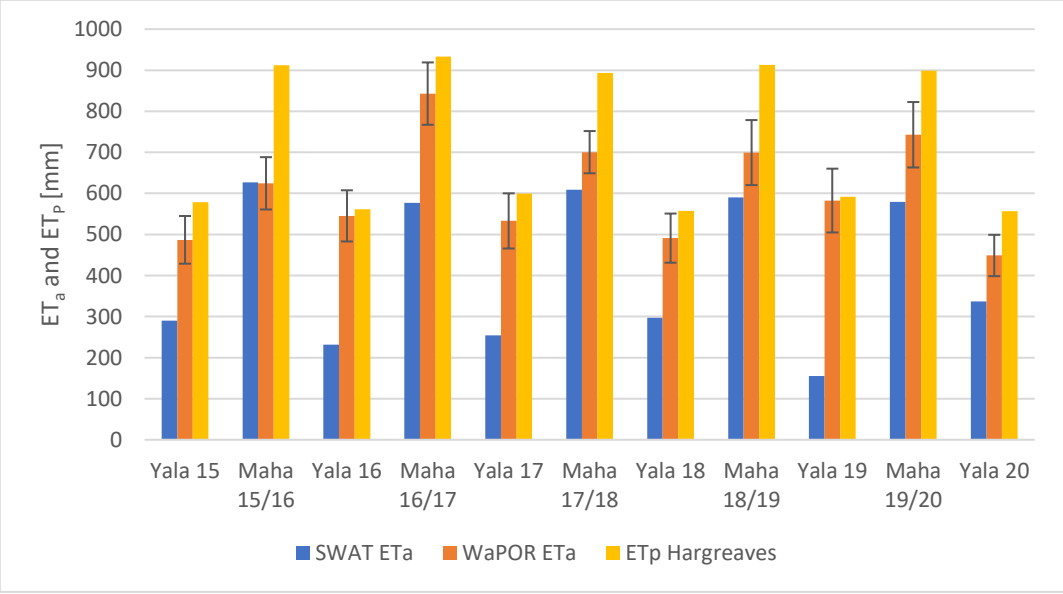

Figure 11: SWAT and WaPOR ET_a compared to ET_p Hargreaves for the Maha and Yala seasons between 2015-2020, the WaPOR ET_a is shown with standard deviation.

The total sums for the *Maha* and *Yala* seasons between 2015-2020 for the parameters presented in Figures 10 and 11 are listed in Table 13. The total difference in ET_a between SWAT and WaPOR is 628 mm for the *Maha* seasons and 1522 mm for the *Yala* seasons. For the *Maha* seasons SWAT ET_a is 83 % of WaPOR ET_a and for the Yala seasons SWAT ET_a is 51 % of WaPOR ET_a, and in total between 2015-2020 SWAT ET_a is 68 % of WaPOR ET_a. The ratio between ET_a and precipitation is 0.65 and 0.85 for SWAT, and 0.78 and 1.68 for WaPOR for the *Maha* and *Yala* seasons, respectively, and the ratio of the total sum is 0.70 for SWAT and 1.04 for WaPOR. The high ratio of WaPOR ET_a to precipitation in the *Yala* seasons could be explained by a high amount of irrigation, more so than in the *Maha* seasons, which also is shown when comparing the seasons to ET_p in Figure 11.

The ratio between ET_a and ET_p Hargreaves is 0.66 and 0.45 for SWAT for the *Maha* and *Yala* seasons respectively, and 0.79 and 0.90 for WaPOR. The ratio of the total ET_a and ET_p Hargreaves between 2015-2020 is 0.57 for SWAT and 0.84 for WaPOR.

Table 13: Summation of the SWAT ET_a, WaPOR ET_a, ET_p Hargreaves, and precipitation for the Maha and Yala seasons between 2015-2020 and the total sum.

Year (2015-2020)	**SWAT ET_a (mm)**	**WaPOR ET_a (mm)**	**ET_p Hargreaves (mm)**	**Precipitation (mm)**
Sum Maha	2982	3610	4551	4610
Sum Yala	1565	3087	3445	1841
Total sum	4547	6697	7996	6451

The ET_a validation based on land use class in Figure 12 presents the SWAT HRUs with the same land use class and the aggregated WaPOR cell values per year. The distribution of the 207 HRUs per land use class was the following: 86 FRSD (deciduous forest), 48 RICE (rice), 72 RNGE (range grass), and 1 WATR (water).

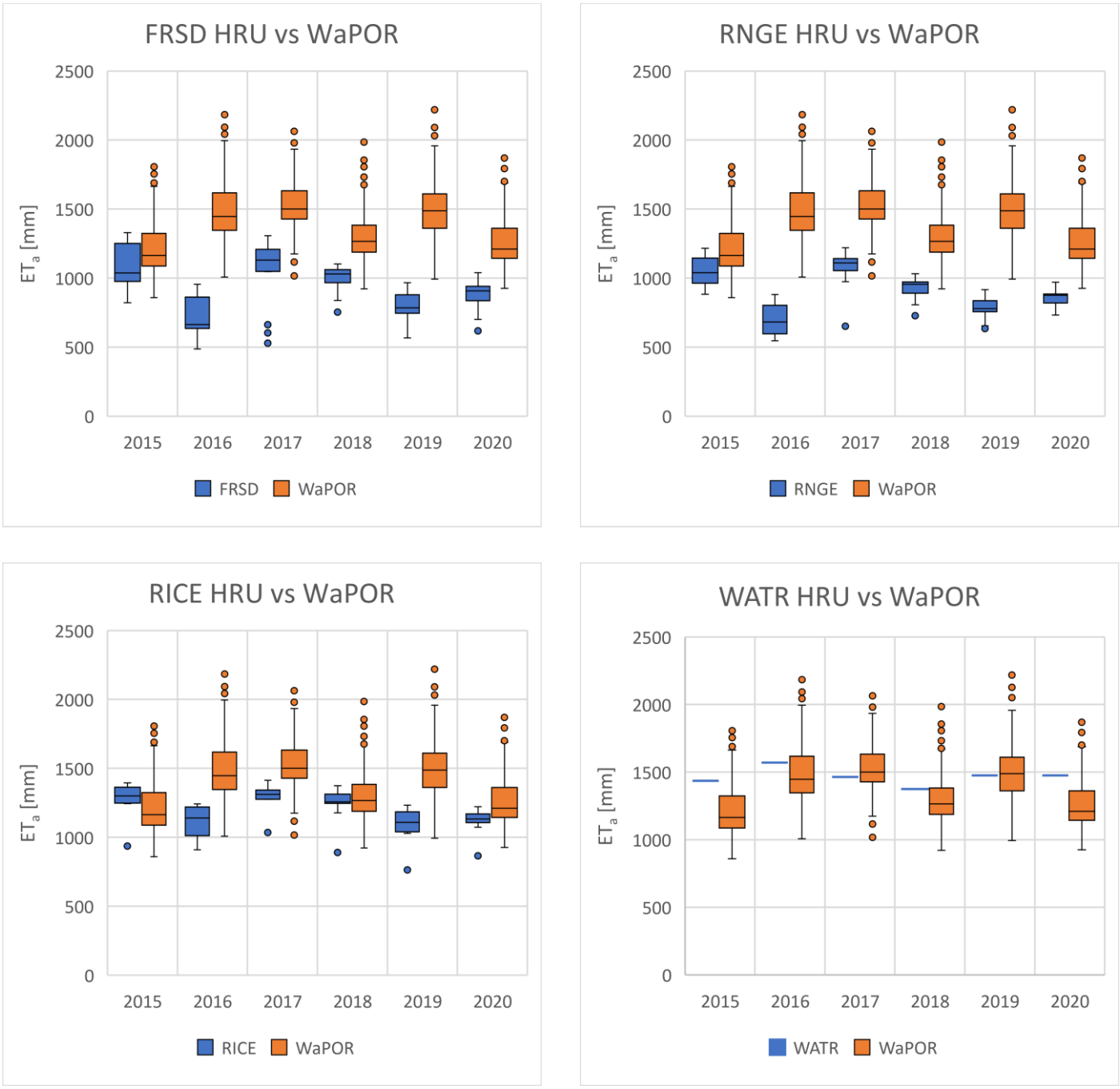

Figure 12: Annual comparison of the ET_a from HRUs with the same land use class and WaPOR ET_a pixel values in the Malwathu Oya river basin. FRSD, RICE, RNGE, and WATR denote the SWAT land use classes and represent deciduous forest, rice, range grasses, and water bodies, respectively.

The FRSD and RNGE HRUs are displaying similar patterns compared to WaPOR, and for all years except 2015 there is not much correlation between the data sets. The RICE HRUs that were auto irrigated show a good correlation with WaPOR in 2018 where the boxes match well, in 2015 SWAT's box is partly matching WaPOR's with the upper quartile being over WaPOR's, and in 2020 SWAT partly

matches WaPOR's box in the lower quartile. Except those three years SWAT is underpredicting ET_a compared to WaPOR, however with a smaller difference for the RICE HRUs compared to FRSD and RNGE. The WATR HRU displayed a better correlation with WaPOR with the ET_a values being within the lower and upper quartile for the years 2016-2019 indicating that WaPOR's ET_a correlates well with SWAT for water bodies i.e., unlimited water supply.

The low ET_a for the FRSD and RNGE could partially be explained by a dormancy period for 10 days between day 352-361 that was simulated by SWAT every year. This happens automatically in the model when a certain day length threshold is reached. During this dormancy period the plants lose 0.3 of their biomasses by default.

The mean annual ET_a for WaPOR, SWAT, and the different HRUs (Table 14) between 2015-2020 is showing a difference between WaPOR and SWAT of 438 mm and the difference of WaPOR and RICE was 176 mm which was the land use HRU that was most equal to WaPOR except the WATR HRUs.

Table 14: Mean annual ET_a for the years 2015-2020 for SWAT, WaPOR, and the different HRUs.

Level	Basin	Basin	HRU	HRU	HRU	HRU
Data	WaPOR	SWAT	FRSD	RNGE	RICE	WATR
Mean ET_a (mm y^{-1})	1368	930	925	897	1192	1466
Standard deviation (mm y^{-1})	130	122	137	131	85	58

From the SWAT output.hru file the average water stress days per month and season were analysed (Table 15). This shows that the FRSD HRUs were the most water stressed with 7.5 water stress day/month in the *Maha* season and 14.8 water stress days/month in the *Yala* season. For the RNGE HRUs the water stress was less with 3.6 water stress days/month for both seasons, and for the RICE HRUs the water stress days/month were 0.39 and 0.45 for *Maha* and *Yala* respectively, thus showing that the auto irrigation worked.

Table 15: Average water stress days per month for the Maha and Yala seasons for the FRSD, RNGE and RICE HRUs.

HRU	FRSD	RNGE	RICE
Maha (water stress days/month)	7.5	3.6	0.39
Maha STD (water stress days/month)	1.0	0.6	0.12
Yala (water stress days/month)	14.8	3.6	0.45
Yala STD (water stress days/month)	4.1	3.5	0.09

5. Discussion

5.1. Sensitivity Analysis and Calibration

The three parameters that were the most sensitive to streamflow calibration were the curve number for moisture condition II (CN2), the soil available water capacity (SOL_AWC), and the soil evaporation compensation factor (ESCO). CN2 estimates the runoff based on antecedent soil water conditions, land use, and soil permeability, thus estimating the amount of runoff water that eventually will reach the stream, so it is reasonable that it is the most sensitive parameter. The SOL_AWC is determining how much water the soil is holding, therefore the runoff is dependent on this parameter since that will determine the amount of water that can infiltrate into the soil or become runoff. The ESCO parameter determines how much of the soil evaporative demand that can be extracted from deeper soil layers and is therefore not as directly related to streamflow creating processes. It is however also affecting the soil water content throughout the soil profiles which in turn reflects how much water turns to runoff, lateral flow to the stream, or groundwater contributing to stream flow. In comparison with other studies that have calibrated SWAT against streamflow with SUFI-2 in both similar climates and different, CN2 is most of the time the top-3 most sensitive parameter (Narsimlu et al. 2015; Khalid et al. 2016; Mehan et al. 2017; Mengistu et al. 2019; Odusanya et al. 2021), SOL_AWC was the most sensitive parameter in (Mehan et al. 2017) and ranked as the 5th most sensitive parameter in (Khalid et al. 2016). When ESCO was included in the above-mentioned studies it ranked 5th and 7th. The CN2 parameter can thus be regarded as a consistently sensitive parameter for streamflow.

However, the parameters that are sensitive to streamflow are not necessarily the same parameters that are sensitive to ET_a. In the studies by Sirisena et al. (2020) and Odusanya et al. (2021) a SWAT model was calibrated in SWAT-CUP using either streamflow data or RS derived ET_a data and the results showed that the sensitivity ranking of the parameters differed between the two methods. In Odusanya et al. (2021) the parameters EPCO (plant uptake compensation factor), CANMX (maximum canopy storage), and SOL_BD (soil bulk density) were the three most sensitive for ET_a and CN2 and ESCO were ranked as number 4 and 5. Sirisena et al. (2020) found that SOL_BD, SOL_Z (depth from soil surface to bottom of layer), ESCO, EPCO, and SOL_AWC were the most sensitive for ET_a. This shows the difference between the parameter sensitivities if one calibrates against streamflow or ET_a. Therefore, an improvement would be to measure the most sensitive parameters for ET_a in the field.

The calibrated value that was most notable was the SOL_AWC that was very high compared to Mapa & Pathmarajah (1995) study in the dry zone. Even though this value gives a good, simulated result for the streamflow calibration it does not mean that it is reflecting the real conditions. The goal with the calibration algorithm is to find the best simulation to maximize the objective function, in this case NSE, the actual calibrated values might therefore not necessarily reflect the real conditions, as long as the objective function is maximized the calibration has found the best solution. The second or third best simulation could also be achieving a satisfactory result not significantly worse than the best simulation. These could have a different combination of parameter values but still achieve a similar result which is worth to keep in mind.

The evaluation coefficients for the calibration were all satisfactory (Moriasi et al. 2007) with R^2 0.72, NSE 0.69, and PBIAS -10.4. The PBIAS value is indicating that the simulation has an overestimation bias which can be seen from the hydrograph (Figure 8) where the baseflow and the smaller peaks during baseflow are overestimated. An increased water uptake from the vegetation could improve this. From the bigger rainfall events two peaks are skewed which probably is due to the rainfall data, trying two adjust only these two would affect all the other peaks which are not showing the same behaviour. The biggest peak in the middle of the simulation period is where a lot of discharge is not captured. The simulated value is about half of the observed, improving this peak would increase the NSE notably.

The p-factor and r-factor which are the evaluation coefficients of the 95PPU had the values of 0.66 and 0.68, respectively. The p-factor could be increased by a better estimation of the baseflow and a better capture of the biggest discharge peak. By doing a more manual change of the parameter ranges in the calibration and not decreasing the range too much i.e., the r-factor could improve the results.

5.2. Water Balance Components

It was found that the ratio between ET_a and precipitation was 0.68 as an annual average between 2012-2020 with ET_a being 922 mm y^{-1} and precipitation 1361 mm y^{-1}. The surface runoff to precipitation ratio was 0.19. In a study by Bastiaanssen & Chandrapala (2003) the corresponding values in the Malwathu Oya river basin between June 1999-2000 were found to be 1223 mm y^{-1} of precipitation and 1290 mm y^{-1} of ET_a giving a ratio of 1.05. The surface runoff to precipitation ratio was 0.29. Both the ratios in this study are therefore comparatively low, especially the ET_a to precipitation ratio. Since the precipitation values are quite similar it means that the partitioning between the water balance components is very different and, in this study, more of the water is being recharged to the shallow and deep aquifers

that is not taking part in any ET processes. And since the ET_a to precipitation ratio was >1 in Bastiaanssen & Chandrapala (2003) it also means that water probably was evapotranspired by plant uptake from shallow groundwater, this does not appear to be the case in this study. The study period between June 1999-2000 is however a short period of time so the values could differ on a larger timescale.

5.3. Comparison of SWAT ET_a with WaPOR ET_a

SWAT was showing an underprediction compared to WaPOR for most of the seasons, especially in the *Yala* seasons where the difference was 200-300 mm per season for some seasons. SWAT's behaviour follows the precipitation pattern, in the *Maha* seasons when the rainfall is a lot higher than in the *Yala* seasons SWAT also shows more similar values compared to WaPOR. The reasons for why SWAT is unable to simulate higher ET_a during low rainfall periods is obviously due to lack of water in the model. This is shown by the amount of water stress days for especially the FRSD HRUs in Table 15. Some explanations for this is that the SWAT model is not representing the water that the vegetation is absorbing from the shallow aquifers which prevents water stress during dry periods. Bastiaanssen & Chandrapala (2003) stated that the forest in the dry zone stands in a seepage zone and is probably extracting water directly from the shallow aquifer and is thus not greatly water stressed during dry periods. This would probably account for a big part of the missing ET_a in the *Yala* seasons, especially since the forest cover is 63.7 % of the river basin area. By not using the default parameters for deciduous forest in the model and instead using measured forest parameters would allow the model to represent the real conditions better.

A further reason for the underestimation by SWAT is the dormancy period that SWAT by default makes the plant enter if a certain day light threshold is reached. This occurred for 10 days for the RNGE and FRSD HRUs. The period isn't that long but the plants in these HRUs lost 0.30 of their above ground biomasses during this period. This would mean a noticeable loss of transpiration before the plants have regrown the lost biomass. The dormancy occurred at the end of the year between days 352-361 so this would affect the ET_a during the Maha seasons. Since there is no natural dormancy in the climate of Sri Lanka it is not representing the system accurately. The reason for the default dormancy period is because SWAT originally was developed for temperate climates. Efforts have been made to adjust the SWAT model to better represent perennial plants in tropical climates that do not undergo dormancy. Strauch & Volk (2013) developed a plant growth modification to address this issue and Arroio Júnior (2017) overcame this problem by making changes in the source code, methods that due to time constraint could not be tested in this study. Another limitation with the plants is that only the RICE land use was

improved with measured values, the RNGE and FRSD land use classes were only using the default values from the SWAT database. A better representation of these land use classes could therefore also affect the amount of water that is taken up by the plants and the ET_a.

The SWAT model was calibrated against observed discharge data and as mentioned in the discussion on the calibration the parameters that are sensitive to streamflow differ to the ones that are sensitive to ET_a (Sirisena et al. 2020; Odusanya et al. 2021). These studies also showed that the SWAT models that were calibrated with discharge performed satisfactorily at simulating streamflow but not ET_a, and the model calibrated with ET_a performed satisfactorily when simulating ET_a but not discharge. Hence, a calibration with ET_a would probably improve the performance of the model in this case.

Another limitation with the SWAT model is the input data. The rainfall data that was used had gaps of <10 % which were accounted for with linear regression gap filling. The uncertainty in this data makes the ET_a prediction less reliant. As could be seen in the hydrograph during calibration a couple of delays in the peak rainfall events and one extra peak of rainfall were observed, signs that the rainfall is not always representing the system accurately. Moreover, the soil map that was used was of very coarse resolution and the field measurements were only conducted in one small area of one of the soil classes. To improve the model further field data measurements would have to be taken in a greater area extent and by using a soil map with higher resolution since the soil input data are of high importance when modelling the land-surface hydrology as it determines the flow of water both on land and in the ground.

To find out whether SWAT or WaPOR represents the ET_a in the river basin better it can be compared with other studies that have analysed the water balance in Sri Lanka and specifically in the dry zone. From the Figures 10 and 11 the ET_a of both methods is compared to the precipitation and the ET_p. The ratios between ET_a and precipitation and the difference between ET_a and ET_p are what can be analysed to determine this. In the study by Bastiaanssen & Chandrapala (2003) where a water balance analysis on a national scale in Sri Lanka was performed it was found that the dry monsoon forest (which is comparable to the forest in this study) was having an ET_a of 1407 mm y^{-1} between June 1999 – 2000 with a precipitation of 1345 mm y^{-1}, hence a deficit of 62 mm. And for the paddy areas, although accounted for all paddy fields in the whole country had an ET_a of 1226 mm y^{-1} with 1665 mm y^{-1} precipitation during the same time period, that is a surplus of 439 mm. In this study the rainfall was on average 1361 mm y^{-1} between 2010-2020 and the FRSD HRUs had an average ET_a of 925 mm y^{-1} and the RICE HRUs 1192 mm y^{-1}. WaPOR had

for the whole basin an estimated annual average of 1368 mm y^{-1} so in comparison to Bastiaanssen & Chandrapala (2003) the SWAT RICE HRUs are performing well but the FRSD HRUs are highly underestimated. WaPOR has an average ET_a value that corresponds quite well to both the land uses.

Furthermore, Bastiaanssen & Chandrapala (2003) showed that roughly half of the Malwathu Oya river basin had a water deficit, i.e., (precipitation – $ET_a < 0$), of 0 – 500 mm, and a smaller area being 500 – 1000 mm, for the period June 1999 – 2000, for the most part in the downstream area, while the upstream half of the basin had a surplus of 0 – 500 mm. The deficit was explained by that the perennial vegetation in those areas is tapping the shallow aquifers directly or indirectly through capillary rise (Bastiaanssen & Chandrapala 2003). Thus, in comparison to that WaPOR is with a deficit of (1361 mm y^{-1} precipitation – 1368 mm y^{-1} ET_a = -7 mm y^{-1}) representing the average quite well while SWAT's average ET_a for the whole basin is 930 mm y^{-1}, giving a surplus of (1361 mm y^{-1} precipitation – 930 mm y^{-1} ETa = 430 mm y^{-1}), thus in the upper range compared to Bastiaanssen & Chandrapala (2003). The study period in Bastiaanssen & Chandrapala (2003) is however a very short period for a hydrological assessment so the comparisons may not be valid on a longer time scale. Moreover, WaPOR has also got uncertainties, one of them being the occurrence of cloud cover which is frequent in the monsoonal climate of Sri Lanka. This leads to lower quality NDVI data as gap filling is done (FAO 2020a), thus leading to less secure ET_a estimates. WaPOR has previously been known to overestimate ET_a (although in Africa) and especially in dry and hot water stressed conditions and in irrigated fields (Blatchford et al. 2020; FAO 2020b). This can be an explanation for the high values compared to SWAT in this study. More information of WaPOR's performance in Sri Lanka is however needed to conclude whether SWAT or WaPOR is the better option for estimating ET_a in the Malwathu Oya river basin.

6. Conclusions

The SWAT model was used in this study to assess the water balance in the Malwathu Oya river basin, Sri Lanka, and showed that ET_a was 68 % of the precipitation as an annual average between 2012-2020. The model was calibrated with a satisfactory result against streamflow and the three most sensitive parameters were CN2, SOL_AWC, and ESCO. The SWAT ET_a was compared to the RS derived ET_a from WaPOR. The results showed that SWAT underestimated ET_a compared to WaPOR during both growing seasons, although particularly in the *Yala* season which receives less rainfall. However, the SWAT HRUs with the auto-irrigated rice agreed well with WaPOR for several years while the forest and range-grass HRUs were underpredicted. The lack of ET_a in the SWAT model was explained by insufficient representation of water being extracted from the shallow aquifer by the plants, a dormancy period, and calibration against streamflow instead of ET_a. To improve the performance of the SWAT model in simulating ET_a the following recommendations are given:

- Improvement and validation of groundwater processes such as the simulation of shallow aquifers. These play a vital role in the Malwathu Oya river basin since the forest is extracting a lot of this water, particularly in the drier *Yala* season. More accurate forest parameters are therefore needed to simulate this.

- Using methods to cope with the default dormancy period in SWAT which is not naturally occurring in the tropics. Previous studies have shown ways to achieve this (Strauch & Volk 2013; Arroio Júnior 2017).

- Streamflow calibration to estimate ET_a in SWAT has previously been tested and has not been optimal (Sirisena et al. 2020; Odusanya et al. 2021). Instead, calibration should be performed with ET_a considering the different sensitivities of the parameters driving the two processes.

- Implementation of a higher resolution soil map along with more soil measurements in the river basin.

References

Abbaspour, K.C. (2015). SWAT-CUP: SWAT Calibration and Uncertainty Programs - A User Manual. Swiss Federal Institute of Aquatic Science and Technology.

Abbaspour, K.C., Johnson, C.A. & van Genuchten, M.Th. (2004). Estimating Uncertain Flow and Transport Parameters Using a Sequential Uncertainty Fitting Procedure. *Vadose Zone Journal*, 3 (4), 1340–1352. https://doi.org/10.2136/vzj2004.1340

Abbaspour, K.C., Yang, J., Maximov, I., Siber, R., Bogner, K., Mieleitner, J., Zobrist, J. & Srinivasan, R. (2007). Modelling hydrology and water quality in the pre-alpine/alpine Thur watershed using SWAT. *Journal of Hydrology*, 333 (2), 413–430. https://doi.org/10.1016/j.jhydrol.2006.09.014

Allen, R., Pereira, L., Raes, D. & Smith, M. (1998). FAO Irrigation and drainage paper No. 56. *Rome: Food and Agriculture Organization of the United Nations*, 56, 26–40

Arnold, J.G., Kiniry, J.R., Srininvasan, R., Williams, J.R., Haney, E.B. & Neitsch, S.L. (2012). Soil and Water Assessment Tool, Input/Output Documentation Version 2012. Texas Water Resource Institute.

Arroio Júnior, P.P. (2017). *Aprimoramento das rotinas e parâmetros dos processos hidrológicos do modelo computacional Soil and Water Assessment Tool - SWAT*. (Doutorado em Ciências da Engenharia Ambiental). Universidade de São Paulo. https://doi.org/10.11606/T.18.2017.tde-25052017-084925

ASTM (2009). Standard Test Method for Infiltration Rate of Soils in Field Using Double-Ring Infiltrometer 1. https://www.academia.edu/30581105/Standard_Test_Method_for_Infiltration_Rate_of_Soils_in_Field_Using_Double_Ring_Infiltrometer_1 [2022-04-10]

Bastiaanssen, W.G.M. & Chandrapala, L. (2003). Water balance variability across Sri Lanka for assessing agricultural and environmental water use. *Agricultural Water Management*, 58 (2), 171–192. https://doi.org/10.1016/S0378-3774(02)00128-2

Bastiaanssen, W.G.M., Cheema, M.J.M., Immerzeel, W.W., Miltenburg, I.J. & Pelgrum, H. (2012). Surface energy balance and actual evapotranspiration of the transboundary Indus Basin estimated from satellite measurements and the ETLook model. *Water Resources Research*, 48 (11). https://doi.org/10.1029/2011WR010482

Beven, K.J. (2020). hydrologic sciences. Encyclopedia Britannica. https://www.britannica.com/science/hydrologic-sciences [2022-02-02]

Blatchford, M.L., Mannaerts, C.M., Njuki, S.M., Nouri, H., Zeng, Y., Pelgrum, H., Wonink, S. & Karimi, P. (2020). Evaluation of WaPOR V2 evapotranspiration products across Africa. *Hydrological Processes*, 34 (15), 3200–3221. https://doi.org/10.1002/hyp.13791

Brouwer, C., Prins, K. & Heibloem, M. (1989). Irrigation Water Management: Training Manual No. 4: Irrigation scheduling. https://www.fao.org/3/t7202e/t7202e00.htm#Contents [2022-05-19]

Brutsaert, W. & York, W. (Cornell U.B., New (2005). *Hydrology: An Introduction*. Cambridge University Press.

Cowan, I.R. (1978). Stomatal Behaviour and Environment. *Advances in Botanical Research*. Elsevier, 117–228. https://doi.org/10.1016/S0065-2296(08)60370-5

Department of Agriculture Sri Lanka (2021). *Irrigation requirement and frequency*. *RICE IN SRI LANKA-WATER MANAGEMENT*. https://doa.gov.lk/rrdi_watermanagement_irrigationrequirement/ [2022-05-19]

Department of Census and Statistics (n.d.). *Paddy Statistics*. *Department of Census and Statistics*. http://www.statistics.gov.lk/Agriculture/StaticalInformation/rubpaddy [2021-11-02]

van Dijk, A.I.J.M. & Renzullo, L.J. (2011). Water resource monitoring systems and the role of satellite observations. *Hydrology and Earth System Sciences*, 15 (1), 39–55. https://doi.org/10.5194/hess-15-39-2011

Eijkelkamp, G., The Netherlands (2018). Double-Ring Infiltrometer—Operating Instructions. https://www.eijkelkamp.com/download.php?file=M0904e_Double_ring_infiltrometer_ac22.pdf [2022-04-10]

FAO (2020a). *WaPOR database methodology: Version 2 release, April 2020*. Rome, Italy: FAO. https://doi.org/10.4060/ca9894en

FAO (2020b). *WaPOR V2 quality assessment: Technical report on the data quality of the WaPOR FAO database version 2*. Rome, Italy: FAO. https://doi.org/10.4060/cb2208en

FAO (n.d.a). *Background and challenges*. https://www.fao.org/in-action/knowat/country-activities/sri-lanka/background-and-challenges/en/ [2021-11-29]

FAO (n.d.b). *Introduction | WaPOR, remote sensing for water productivity | Food and Agriculture Organization of the United Nations*. https://www.fao.org/in-action/remote-sensing-for-water-productivity/wlpa-introduction/introduction/en/ [2022-01-30]

García, L., Rodríguez, J.D., Wijnen, M. & Pakulski, I. (2016). *Earth Observation for Water Resources Management: Current Use and Future Opportunities for the Water Sector*. Washington, DC: World Bank. https://doi.org/10.1596/978-1-4648-0475-5

Gassman, P.W., Sadeghi, A.M. & Srinivasan, R. (2014). Applications of the SWAT Model Special Section: Overview and Insights. *Journal of Environmental Quality*, 43 (1), 1–8. https://doi.org/10.2134/jeq2013.11.0466

Geekiyanage, N. & Pushpakumara, D.K.N.G. (2013). Ecology of ancient Tank Cascade Systems in island Sri Lanka. *Journal of Marine and Island Cultures*, 2 (2), 93–101. https://doi.org/10.1016/j.imic.2013.11.001

Gelcer, E., Fraisse, C. & Sentelhas, P. (2010). Evaluation of Methodologies to Estimate Reference Evapotranspiration in Florida., January 1 2010.

Hargreaves, G. & Samani, Z. (1985). Reference Crop Evapotranspiration From Temperature. *Applied Engineering in Agriculture*, 1. https://doi.org/10.13031/2013.26773

Harischandra, I., Dassanayake, R. & De Silva, N. (2016). Three sympatric clusters of the malaria vector Anopheles culicifacies E (Diptera: Culicidae) detected in Sri Lanka. *Parasites & Vectors*, 9. https://doi.org/10.1186/s13071-015-1286-3

Iresh, S., Marasinghe, A., Wedanda, A., Wickramasekara, G., Wickramasooriya, M., & Premathilake (2021). Development of a Hydrological Model for Kala Oya Basin Using SWAT Model. *Engineer - Journal of the Institution of Engineers, Sri Lanka*, 54, 2021

J. G. Arnold, D. N. Moriasi, P. W. Gassman, K. C. Abbaspour, M. J. White, R. Srinivasan, C. Santhi, R. D. Harmel, A. van Griensven, M. W. Van Liew, N. Kannan, & M. K. Jha (2012). SWAT: Model Use, Calibration, and Validation. *Transactions of the ASABE*, 55 (4), 1491–1508. https://doi.org/10.13031/2013.42256

Jensen, M.E., Burman, R.D., Allen, R.G. & American Society of Civil Engineers (eds.) (1990). *Evapotranspiration and irrigation water requirements: a manual*. New York, N.Y: The Society. (ASCE manuals and reports on engineering practice; no. 70)

Kaur, A. & Fanourakis, G. (2018). Effect of Sodium Carbonate Concentration in Calgon on Hydrometer Analysis Results. *Periodica Polytechnica Civil Engineering*, 62. https://doi.org/10.3311/PPci.9424

Khalid, K., Ali, M.F., Rahman, N.F.A., Mispan, M.R., Haron, S.H., Othman, Z. & Bachok, M.F. (2016). Sensitivity Analysis in Watershed Model Using SUFI-2 Algorithm. *Procedia Engineering*, 162, 441–447. https://doi.org/10.1016/j.proeng.2016.11.086

Kirschbaum, M.U.F. (2004). Direct and Indirect Climate Change Effects on Photosynthesis and Transpiration. *Plant Biology*, 6 (3), 242–253. https://doi.org/10.1055/s-2004-820883

Kumar, D.N. & Reshmidevi, T.V. (2013). Remote Sensing Applications in Water Resources. *Journal of the Indian Institute of Science*, 93 (2), 163–188

Lehner, B., Verdin, K. & Jarvis, A. (2008). New global hydrography derived from spaceborne elevation data. Eos, Transactions, 89(10): 93-94. https://www.hydrosheds.org/

Longman, R.J., Newman, A.J., Giambelluca, T.W. & Lucas, M. (2020). Characterizing the Uncertainty and Assessing the Value of Gap-Filled Daily Rainfall Data in Hawaii. *Journal of Applied Meteorology and Climatology*, 59 (7), 1261–1276. https://doi.org/10.1175/JAMC-D-20-0007.1

Mapa, R.B. & Pathmarajah, S. (1995). Contrasts in the physical properties of three soils of an Alfisol catena in Sri Lanka. *Soil Use and Management*, 11 (2), 90–93. https://doi.org/10.1111/j.1475-2743.1995.tb00502.x

Mehan, S., Neupane, R.P. & Kumar, S. (2017). Coupling of SUFI 2 and SWAT for Improving the Simulation of Streamflow in an Agricultural Watershed of South Dakota. *Hydrology: Current Research*, 08 (03). https://doi.org/10.4172/2157-7587.1000280

Mengistu, A.G., van Rensburg, L.D. & Woyessa, Y.E. (2019). Techniques for calibration and validation of SWAT model in data scarce arid and semi-arid catchments in South Africa. *Journal of Hydrology: Regional Studies*, 25, 100621. https://doi.org/10.1016/j.ejrh.2019.100621

Monteith, J.L. & Unsworth, M.H. (2013). *Principles of environmental physics: plants, animals, and the atmosphere*. 4th ed. Amsterdam ; Boston: Elsevier/Academic Press.

Moriasi, D., Arnold, J., Van Liew, M., Bingner, R., Harmel, R.D. & Veith, T. (2007). Model Evaluation Guidelines for Systematic Quantification of Accuracy in Watershed Simulations. *Transactions of the ASABE*, 50. https://doi.org/10.13031/2013.23153

Munn, R.E. (ed.) (2002). *Encyclopedia of global environmental change*. Chichester ; New York: Wiley.

Muthuwatta, L., Perera, H.P.T.W., Eriyagama, N., Upamali Surangika, K.B.N. & Premachandra, W.W. (2017). Trend and variability of rainfall in two river basins in Sri Lanka: an analysis of meteorological data and farmers' perceptions. *Water International*, 42 (8), 981–999. https://doi.org/10.1080/02508060.2017.1406784

Narsimlu, B., Gosain, A.K., Chahar, B.R., Singh, S.K. & Srivastava, P.K. (2015). SWAT Model Calibration and Uncertainty Analysis for Streamflow Prediction in the Kunwari River Basin, India, Using Sequential Uncertainty Fitting. *Environmental Processes*, 2 (1), 79–95. https://doi.org/10.1007/s40710-015-0064-8

Neitsch, S., Arnold, J., Kinry, J.R. & Williams, J.R. (2011). Soil and water assessment tool theoretical documentation. *Version*,

Null, N., Jensen, M.E. & Allen, R.G. (2016). *Evaporation, Evapotranspiration, and Irrigation Water Requirements*. American Society of Civil Engineers. https://doi.org/10.1061/9780784414057

Odusanya, A.E., Schulz, K., Biao, E.I., Degan, B.A.S. & Mehdi-Schulz, B. (2021). Evaluating the performance of streamflow simulated by an eco-hydrological model calibrated and validated with global land surface actual evapotranspiration from remote sensing at a catchment scale in West Africa. *Journal of Hydrology: Regional Studies*, 37, 100893. https://doi.org/10.1016/j.ejrh.2021.100893

Panabokke, C.R., Sakthivadivel, R. & Weerasinghe, A.D. (2002). *Small tanks in Sri Lanka: evolution, present status, and issues*. Colombo: International Water Management Institute.

Pörtner, H.-O., Roberts, D.C., Tignor, M., Poloczanska, E.S., Mintenbeck, K., Alegría, A., Craig, M., Langsdorf, S., Löschke, S., Möller, V., Okem, A., Rama, B. & (eds.) (2022). *IPCC, 2022: Climate Change 2022: Impacts, Adaptation, and Vulnerability. Contribution of Working Group II to the Sixth Assessment Report of the Intergovernmental Panel on Climate Change*. Cambridge University Press. In Press.

Rosemary, F., Vitharana, U.W.A., Indraratne, S.P., Weerasooriya, R. & Mishra, U. (2017). Exploring the spatial variability of soil properties in an Alfisol soil catena. *CATENA*, 150, 53–61. https://doi.org/10.1016/j.catena.2016.10.017

Seenithamby, M. & Nandalal, K.D.W. (2021). Water resource development planning around village cascades: piloting of a scientific methodology in Yan Oya river basin of Sri Lanka. *Water Policy*, 23 (4), 946–969. https://doi.org/10.2166/wp.2021.098

Sheffield, J., Wood, E.F., Pan, M., Beck, H., Coccia, G., Serrat-Capdevila, A. & Verbist, K. (2018). Satellite Remote Sensing for Water Resources Management: Potential for Supporting Sustainable Development in Data-Poor Regions. *Water Resources Research*, 54 (12), 9724–9758. https://doi.org/10.1029/2017WR022437

Sirisena, T.A.J.G., Maskey, S. & Ranasinghe, R. (2020). Hydrological Model Calibration with Streamflow and Remote Sensing Based Evapotranspiration Data in a Data Poor Basin. *Remote Sensing*, 12 (22), 3768. https://doi.org/10.3390/rs12223768

Sivakumar, S., S.S., S. & T, T. (2019). OPERATIONAL POLICY OF THE RESERVOIRS IN MALWATHU OYA RIVER BASIN TO MINIMIZE FLOOD DAMAGES IN ANURADHAPURA, VAVUNIYA AND MANNAR DISTRICTS IN NORTHERN SRI LANKA.

Sivaprakasam, s. D., Alagappan, M. & Mohan, S. (2011). Modified Hargreaves Equation for Estimation of ET0 in a Hot and Humid Location in Tamilnadu State, India. *International Journal of Engineering Science and Technology*, 3

Soil Conservation Service Engineering Division (1986). *Urban Hydrology for Small Watersheds*. (Technical Release 55). U.S. Department of Agriculture. https://www.nrcs.usda.gov/Internet/FSE_DOCUMENTS/stelprdb1044171.pdf [2022-05-21]

Strauch, M. & Volk, M. (2013). SWAT plant growth modification for improved modeling of perennial vegetation in the tropics. *Ecological Modelling*, 269, 98–112. https://doi.org/10.1016/j.ecolmodel.2013.08.013

Taiz, L. & Zeiger, E. (2002). *Plant physiology*. 3rd ed. Sunderland, Mass: Sinauer Associates.

Thornthwaite, C.W. (1948). An Approach toward a Rational Classification of Climate. *Geographical Review*, 38 (1), 55–94. https://doi.org/10.2307/210739

Trajkovic, S. (2007). Hargreaves versus Penman-Monteith under Humid Conditions. *Journal of Irrigation and Drainage Engineering*, 133 (1), 38–42. https://doi.org/10.1061/(ASCE)0733-9437(2007)133:1(38)

Ventura, F., Faber, B.A., Bali, K.M., Snyder, R.L., Spano, D., Duce, P. & Schulbach, K.F. (2001). Model for Estimating Evaporation and Transpiration from Row Crops. *Journal of Irrigation and Drainage Engineering*, 127 (6), 339–345. https://doi.org/10.1061/(ASCE)0733-9437(2001)127:6(339)

Willmott, C.J., Rowe, C.M. & Mintz, Y. (1985). Climatology of the terrestrial seasonal water cycle. *Journal of Climatology*, 5 (6), 589–606. https://doi.org/10.1002/joc.3370050602

Zanaga, D., Van De Kerchove, R., De Keersmaecker, W., Souverijns, N., Brockmann, C., Quast, R., Wevers, J., Grosu, A., Paccini, A., Vergnaud, S., Cartus, O., Santoro, M., Fritz, S., Georgieva, I., Lesiv, M., Carter, S., Herold, M., Li, L., Tsendbazar, N.-E., Ramoino, F. & Arino, O. (2021). ESA WorldCover 10 m 2020 v100. Zenodo. https://doi.org/10.5281/zenodo.5571936

Appendix A. Determination of Soil Parameters and Harvest Index

Determination of Bulk Density

The bulk density was determined with the undisturbed core sample method. First, the metal cores that were used were weighed and the diameter and height were determined (Table A1), then they were inserted in a core sampler. The core sampler was hammered into the ground to a depth of 30 cm for all six samples and then withdrawn from the soil carefully. The samples were then taken to the laboratory where they were oven dried for 48 hours at 105 °C. After the drying the core samples were weighed again to obtain the dry soil weight. The bulk density was then calculated by dividing the dry soil weight by the core volume in g/cm^3.

Table A1: Dimensions of the metal cores used for the determination of bulk density.

Height (cm)	Diameter (cm)	Volume (cm^3)
5.1	4.7	88.5
5	4.7	86.7
5	4.7	86.7
5.1	4.6	84.8
5	4.6	83.1
5	4.6	83.1

Determination of Soil Texture

The soil texture or the composition of sand, silt, and clay was determined using the simplified hydrometer method. The soils were sampled using an auger and taken at 30 cm depth. Thereafter, the six samples were air-dried for 24 hours. After drying, 40 g of each sample was added into a 600 ml beaker with 100 ml of Calgon solution (a mix of sodium carbonate and sodium hexametaphosphate (Kaur & Fanourakis 2018)) and 300 ml distilled water and was left to soak overnight.

To determine the oven-dried weight, 10 g of each soil sample was taken and then oven-dried for about 10 hours at 105°C and then weighed to determine the moisture content in each sample. The moisture content was then used to calculate the dry weight of the 40 g soil that was used for each measurement, this was denoted as *W*.

When the Calgon solution of each sample had soaked overnight they were transferred to a cylinder and distilled water was used to fill the level up to the 1-liter mark. Thereafter the opening of the cylinder was covered with a plastic sheet fixed with a rubber band and then the solution was mixed by turning the cylinder

upside down 20 times. The time was noted when the mixing was finished and then a hydrometer was placed in the cylinder after 40 seconds (R_{40s}) and after 2 hours (R_{2h}). The temperature in °C was also noted for each hydrometer reading. A blank sample was also prepared with 100 ml of Calgon solution filled up with distilled water to the 1-liter mark. The blank sample was then mixed using the same method and afterwards the hydrometer reading (R_L) and temperature were noted.

Each hydrometer reading was then corrected by adding a value of 0.36 x (C – 19.4) where C is the temperature in °C. The soil texture was then determined by using Equations (A1, A2, A3).

$$Sand\ \% = 100 - (R_{40s} - R_L)\ \times \frac{100}{W} \quad \text{(A1)}$$

$$Clay\ \% = (R_{2h} - R_L)\ \times \frac{100}{W} \quad \text{(A2)}$$

$$Silt\ \% = 100 - (sand\ \% + clay\ \%) \quad \text{(A3)}$$

The mean soil texture was calculated for all six samples and the textural class was determined with the USDA textural triangle. The permanent wilting point (PWP) and field capacity (FC) were determined with the program "Soil Water Characteristics" from USDA[2] based on the mean texture. The available water capacity (AWC) was derived by Equation A4.

$$AWC = FC - PWP \quad \text{(A4)}$$

Determination of Saturated Hydraulic Conductivity

The soil saturated hydraulic conductivity (K_s) was in this study determined by measuring the infiltration rate with a double ring infiltrometer since the constant infiltration rate is roughly equal to K_s (Eijkelkamp 2018). The double-ring infiltrometer measurement was conducted at one site shown in Figure 4. The soil at the site was undisturbed with some grass on the surface and was located next to some paddy fields.

A double ring infiltrometer consists of two metal cylinders (in this study with ~30 cm and ~55 cm diameter) which were driven 5 cm into the ground with a hammer and then filled with water at the same level in both cylinders. The outer ring acts as a buffer to reduce lateral flow in the soil profile, thus promoting vertical flow underneath the inner ring (ASTM 2009). The change in the water level was measured with a floating device in the inner ring and the water was refilled in both

[2] https://www.ars.usda.gov/research/software/download/?softwareid=492&modecode=80-42-05-10

rings every 5 minutes to keep the water level at a constant height. The time was noted for every decrease of 5 mm and when a constant infiltration rate was achieved the measurements were ended and K_s could be determined in mm/h.

Measurement of Harvest Index

First, a quadratic metal frame with an area of 0.25 m^2 was placed out in the paddy field and all the plants that were inside the frame were collected, including the roots. This was done at three different paddy fields; their locations are shown in Figure 4. The grains were then separated from the plants for each sample and placed in a container. Next, the moisture content of the grains was measured with a moisture meter giving the moisture content in percent, thereafter the grains were dried at room temperature for 48 hours. After the grains had dried the moisture content was measured again. The plant materials and the roots were cut into smaller pieces and placed in a paper bag and were let to oven dry at 60 °C for 48 hours.

The plant materials were weighed after the 48-hour drying and then dried again with 1-hour weighing intervals until the weight was constant (0 % moisture content), this took 2 hours, this was done by students at the Rajarata University.

The HI was calculated as the ratio of grain yield mass at 14 % moisture content to the total biomass weight. The grain yield at 14 % was first calculated using Equations A5 and A6, and then HI was calculated using Equation A7.

$$m_0 = m_x - (m_x \times \frac{x}{100}) \quad \text{(A5)}$$

$$m_{14} = m_0 \times \frac{114}{100} \quad \text{(A6)}$$

$$HI = \frac{m_{14}}{m_{14} + m_{plant}} \quad \text{(A7)}$$

Where m_0 is the grain mass at 0 % moisture content, m_x is the mass of the grains at x % moisture content after drying, m_{14} is the mass of the grains at 14 % moisture content, and m_{plant} is the mass of the dried plant materials at 0 % moisture content.

Appendix B. Crop Parameters for Rice

In Table B1 are the crop parameters defined for rice in the SWAT crop database. Only the maximum rooting depth and harvest index were changed.

Table B1: Crop parameters for rice used in the SWAT model. All values except RDMX (maximum rooting depth) and HVSTI (harvest index) (that were measured) are from the crop database in SWAT (Arnold et al. 2012).

Description	Parameter	Value	Unit	Source
Land cover/plant classification	IDC	Warm season annual	-	(Arnold et al. 2012)
Radiation-use efficiency	BIO_E	22	(kg/ha)/(MJ/m^2)	(Arnold et al. 2012)
Harvest index for optimal growing conditions	HVSTI	0.324	(kg/ha)/(kg/ha)	Measured
Lower limit of harvest index	WSYF	0.25	(kg/ha)/(kg/ha)	(Arnold et al. 2012)
Maximum potential leaf area index (LAI) and two fractions of the max. LAI on the leaf area development curve.	BLAI FRGRW1 LAIMX1 FRGRW2 LAIMX2	5 0.3 0.01 0.7 0.95	- - - - -	(Arnold et al. 2012)
Fraction of the growing season when LAI begins to decline.	DLAI	0.8	-	(Arnold et al. 2012)
Max. canopy height	CHTMX	0.8	Meter	(Arnold et al. 2012)
Max. rooting depth	RDMX	0.11	Meter	Measured
Optimal temperature for plant growth	T_OPT	25	°C	(Arnold et al. 2012)
Minimum temperature for plant growth	T_BASE	10	°C	(Arnold et al. 2012)
Normal fraction of N in yield	CNYLD	0.0136	kg N/kg seed	(Arnold et al. 2012)

Normal fraction of P in yield	CPYLD	0.0013	kg P/kg seed	(Arnold et al. 2012)
Fraction of N and P in the plant at emergence, middle of the season, and at maturity.	PLTNFR1 PLTNFR2 PLTNFR3 PLTPFR1 PLTPFR2 PLTPFR3	0.05 0.02 0.01 0.006 0.003 0.0018	Kg N/kg biomass & Kg P/kg biomass	(Arnold et al. 2012)
Minimum of value the USLE C factor, quantifying the max. decrease possible in erosion for the plant.	USLE_C	0.03	-	(Arnold et al. 2012)
Maximum stomatal conductance	GSI	0.008	m/s	(Arnold et al. 2012)
Rate of decline in radiation -use efficiency (RUE) per unit increase in vapor pressure deficit	WAVP	5	$(kg/ha)/(MJ/m^2)$	(Arnold et al. 2012)
Impact of elevated CO2 concentration on RUE	CO2HI	660	$\mu LCO_2/L$ air	(Arnold et al. 2012)
Biomass-energy ration corresponding to the 2nd point on the RUE curve	BIOEHI	31	-	(Arnold et al. 2012)
Plant residue decomposition coefficient	RSDCO_PL	0.05	-	(Arnold et al. 2012)
Biomass die-off fraction	BM_DIEOFF	0.1	-	(Arnold et al. 2012)
Fraction of maximum stomatal conductance	FRGMAX	0.75	-	(Arnold et al. 2012)
Vapor pressure deficit corresponding to FRGMAX	VPDFR	4	kPa	(Arnold et al. 2012)
Light extinction coefficient	EXT_COEFF	0.35	-	(Arnold et al. 2012)

Appendix C. Calibration Data

Table C1: Monthly average discharge data from January 2012 - September 2020 used in the SWAT-CUP calibration. The data is in the input-format for SWAT-CUP. Data for three months is missing.

Number of data point	Flow_month_year	Discharge (m^3/s)
1	FLOW_OUT_1_2012	11.15
2	FLOW_OUT_2_2012	12.79
3	FLOW_OUT_3_2012	6.39
4	FLOW_OUT_4_2012	7.61
5	FLOW_OUT_5_2012	5.42
6	FLOW_OUT_6_2012	2.65
7	FLOW_OUT_7_2012	1.73
8	FLOW_OUT_8_2012	2.08
9	FLOW_OUT_9_2012	0.79
10	FLOW_OUT_10_2012	23.79
11	FLOW_OUT_11_2012	30.45
13	FLOW_OUT_1_2013	163.76
14	FLOW_OUT_2_2013	27.66
15	FLOW_OUT_3_2013	19.96
16	FLOW_OUT_4_2013	10.68
17	FLOW_OUT_5_2013	9.58
18	FLOW_OUT_6_2013	4.5
19	FLOW_OUT_7_2013	4.58
20	FLOW_OUT_8_2013	2.32
21	FLOW_OUT_9_2013	1.23
22	FLOW_OUT_10_2013	2.28
23	FLOW_OUT_11_2013	7.73
24	FLOW_OUT_12_2013	5.13
25	FLOW_OUT_1_2014	15.04
26	FLOW_OUT_2_2014	3.72
27	FLOW_OUT_3_2014	1.13
29	FLOW_OUT_5_2014	13.74
30	FLOW_OUT_6_2014	1.61
31	FLOW_OUT_7_2014	0.94
32	FLOW_OUT_8_2014	1.33
33	FLOW_OUT_9_2014	4.64
34	FLOW_OUT_10_2014	14.48
35	FLOW_OUT_11_2014	73.01
37	FLOW_OUT_1_2015	17.95
38	FLOW_OUT_2_2015	11.06
39	FLOW_OUT_3_2015	7.72
40	FLOW_OUT_4_2015	18.16
41	FLOW_OUT_5_2015	46.26
42	FLOW_OUT_6_2015	4.98
43	FLOW_OUT_7_2015	4.34
44	FLOW_OUT_8_2015	6.15
45	FLOW_OUT_9_2015	2.99
46	FLOW_OUT_10_2015	20.04
47	FLOW_OUT_11_2015	283.26

48	FLOW_OUT_12_2015	151.83
49	FLOW_OUT_1_2016	42.49
50	FLOW_OUT_2_2016	10.77
51	FLOW_OUT_3_2016	3.52
52	FLOW_OUT_4_2016	5.92
53	FLOW_OUT_5_2016	102.3
54	FLOW_OUT_6_2016	9.63
55	FLOW_OUT_7_2016	5.98
56	FLOW_OUT_8_2016	4.73
57	FLOW_OUT_9_2016	1.72
58	FLOW_OUT_10_2016	0.83
59	FLOW_OUT_11_2016	7.22
60	FLOW_OUT_12_2016	3.9
61	FLOW_OUT_1_2017	4.99
62	FLOW_OUT_2_2017	3.03
63	FLOW_OUT_3_2017	5.79
64	FLOW_OUT_4_2017	2.25
65	FLOW_OUT_5_2017	3.69
66	FLOW_OUT_6_2017	1.26
67	FLOW_OUT_7_2017	0.75
68	FLOW_OUT_8_2017	1.8
69	FLOW_OUT_9_2017	4.15
70	FLOW_OUT_10_2017	3.5
71	FLOW_OUT_11_2017	15.65
72	FLOW_OUT_12_2017	6.26
73	FLOW_OUT_1_2018	3.78
74	FLOW_OUT_2_2018	3.01
75	FLOW_OUT_3_2018	2.98
76	FLOW_OUT_4_2018	3.12
77	FLOW_OUT_5_2018	12.59
78	FLOW_OUT_6_2018	3.9
79	FLOW_OUT_7_2018	2.41
80	FLOW_OUT_8_2018	2.6
81	FLOW_OUT_9_2018	2.75
82	FLOW_OUT_10_2018	32.3
83	FLOW_OUT_11_2018	88.11
84	FLOW_OUT_12_2018	22.6
85	FLOW_OUT_1_2019	9.77
86	FLOW_OUT_2_2019	10.93
87	FLOW_OUT_3_2019	2.62
88	FLOW_OUT_4_2019	4.98
89	FLOW_OUT_5_2019	6.88
90	FLOW_OUT_6_2019	2.61
91	FLOW_OUT_7_2019	2.81
92	FLOW_OUT_8_2019	3.24
93	FLOW_OUT_9_2019	1.58
94	FLOW_OUT_10_2019	17.32
95	FLOW_OUT_11_2019	13.19
96	FLOW_OUT_12_2019	198.37
97	FLOW_OUT_1_2020	10.9
98	FLOW_OUT_2_2020	7.65
99	FLOW_OUT_3_2020	3.57
100	FLOW_OUT_4_2020	4.29
101	FLOW_OUT_5_2020	12.56

102	FLOW_OUT_6_2020	4.14
103	FLOW_OUT_7_2020	6.82
104	FLOW_OUT_8_2020	2.61
105	FLOW_OUT_9_2020	2.05

Table C2: SWAT parameters used in the sensitivity analysis and their initial ranges in SWAT-CUP. The r before the parameter means a relative change was applied by multiplying the existing value by (1 + calibrated value). The v before the parameter means that the existing value was replaced by the calibrated value.

Input parameter	**Description** (Arnold et al. 2012)	**Min**	**Max**
r__CN2.mgt	Initial SCS runoff curve number for moisture condition II	-0.2	0.2
v__GW_DELAY.gw	Groundwater delay time (days)	30.0	450.0
v__ALPHA_BF.gw	Baseflow alpha factor (1/days)	0	1
v__GWQMN.gw	Threshold depth of water in the shallow aquifer required for return flow to occur (mm H_2O)	0	5000
v__GW_REVAP.gw	Groundwater "revap" coefficient	0.02	0.2
v__REVAPMN.gw	Threshold depth of water in the shallow aquifer for "revap" or percolation to the deep aquifer to occur (mm H_2O)	0	500
r__SOL_AWC(1).sol	Available water capacity of the soil layer (1) (mm H_2O/mm soil)	-0.1	1
v__ESCO.hru	Soil evaporation compensation factor	0	1
v__CH_N2.rte	Manning's "n" value for the main channel	0	0.3
v__CH_K2.rte	Effective hydraulic conductivity in main channel alluvium (mm/hr)	0	127
v__ALPHA_BNK.rte	Baseflow alpha factor for bank storage (days)	0	1
r__SOL_K(1).sol	Saturated hydraulic conductivity layer (1) (mm/hr)	-0.99	2
r__SOL_BD(1).sol	Moist bulk density layer (1) (g/cm^3)	-0.25	0.25
r__EPCO.bsn	Plant uptake compensation factor	-0.99	1
r__HRU_SLP.hru	Average slope steepness (m/m)	-0.99	1
r__OV_N.hru	Manning's "n" value for overland flow	-0.99	1
r__SLSUBBSN.hru	Average slope length (m)	-0.99	1
v__SURLAG.bsn	Surface runoff lag coefficient	0.05	24

Table C3: SWAT parameters used in the calibration and their final calibrated values.

Input parameter	**Final calibrated value**
r__CN2.mgt	-0.076
v__GW_REVAP.gw	0.108
r__SOL_AWC(1).sol	0.938
v__ESCO.hru	0.170
v__CH_K2.rte	66.964
v__ALPHA_BNK.rte	0.191
r__HRU_SLP.hru	-0.020